

Domain walls of N=2 supergravity in five dimensions from hypermultiplet moduli spaces

L. Anguelova, C. I. Lazaroiu

*C. N. Yang Institute for Theoretical Physics
SUNY at Stony Brook, NY11794-3840, U.S.A.
anguelov, calin @insti.physics.sunysb.edu*

ABSTRACT: We study domain wall solutions in $d=5$, $N=2$ supergravity coupled to a single hypermultiplet whose moduli space is described by certain inhomogeneous, toric ESD manifolds constructed recently by Calderbank and Singer. Upon gauging a generic $U(1)$ isometry of these spaces, we obtain an infinite family of models whose “superpotential” admits an arbitrary number of isolated critical points. By investigating the associated supersymmetric flows, we prove the existence of domain walls of Randall-Sundrum type for each member of our family, and find chains of domain walls interpolating between various AdS_5 backgrounds. Our models are described by a discrete infinity of smooth and complete one-hypermultiplet moduli spaces, which live on an open subset of the minimal resolution of certain cyclic quotient singularities. These spaces generalize the Pedersen metrics considered recently by Behrndt and Dall’Agata.

Contents

1. Introduction	2
2. Flow equations on toric one-hypermultiplet moduli spaces	6
3. Calderbank-Singer spaces	10
3.1 Minimal resolutions of cyclic quotient singularities	10
3.2 The Calderbank-Singer metrics	12
3.3 Fixed points of $U(1)$ isometries	14
4. Supersymmetric flows on Calderbank-Singer spaces	14
4.1 Critical points of the superpotential	14
4.2 Asymptotic form of the flow equations and divisorial flows	15
4.3 General properties of divisorial flows	17
4.4 Flows of Randall-Sundrum type	20
5. Examples	21
5.1 Models with $k > 1$ for low values of p	21
5.2 The Pedersen-LeBrun metrics	22
5.3 The model $(p,q)=(8,3)$	28
5.4 The model $(p,q)=(21,8)$	31
6. Conclusions	33
A. Relation between different coordinate systems for the Pedersen metrics	34

1. Introduction

Five dimensional gauged supergravity has acquired some phenomenological interest due to several recent developments. The work of [1] showed that the reduction of Horava-Witten theory [2] to five dimensions is a gauged minimal supergravity admitting a BPS saturated domain wall solution which can be identified with the four-dimensional space-time of a strongly-coupled heterotic compactification [3]. Another direction is provided by the AdS/CFT correspondence [4]. In this framework the domain walls of $N = 8$ gauged supergravity have a natural interpretation as renormalization group flows in the corresponding field theory. When an embedding of $N = 2$ supergravity into the $N = 8$ theory is known, the associated domain walls of the $N = 2$ theory acquire an RG flow interpretation¹. Yet another development is the proposal of [5] for an alternative to compactification. This scenario requires a domain wall interpolating between two AdS_5 solutions (of equal vacuum energy density) associated with IR points (critical points for the “superpotential” where the warp factor is exponentially small). Despite intense interest in the subject, there has been limited progress in finding explicit supergravity realizations of such scenarios.

In this regard several no-go theorems were proposed [6, 7, 8], which state that, under certain assumptions, there are no supersymmetric domain wall solutions connecting IR critical points of the supergravity potential. As it turns out, the relevant assumptions *can* be violated once one considers coupling to hypermultiplets. In particular, the recent work of [9] provides a counterexample obtained by coupling the supergravity multiplet to a single hypermultiplet described by a certain non-homogeneous quaternion-Kähler space; in this model, the no-go theorems of [6, 7, 8] do not apply. This underscores the importance of reconsidering the problem in the general context of inhomogeneous hypermultiplet moduli spaces.

As a general rule, however, one knows quite a bit about flows on the vector/tensor multiplet moduli space, but rather little about their hypermultiplet counterpart. The difficulty in the latter case consists mainly in understanding the associated geometry. It is well-known that the hypermultiplet moduli space must be a quaternion-Kähler space of negative scalar curvature. To trust the supergravity approximation, one must restrict to smooth quaternion-Kähler spaces². Even restricting to one hypermultiplet (the focus of the present paper), very little is known explicitly for the generic case. In this

¹It has become customary to use RG flow terminology even when such an embedding is not known, and we shall do so in what follows.

²In principle, one may allow for curvature singularities in the *classical* hypermultiplet moduli space. However, one expects such singularities to be removed by quantum effects, for example if the model under consideration can be realized in string/M-theory.

situation, the quaternion-Kähler condition is equivalent to the requirement that M is Einstein-selfdual (ESD). The simplest negative curvature examples are provided by the homogeneous spaces $SU(2, 1)/U(2)$ (the moduli space of the universal hypermultiplet, i.e. the Bergman metric) and $EAdS_4 = SO(4, 1)/SO(4)$ (the Euclidean version of AdS_4 , also known as the hyperbolic space H^4 or the hyperbolic metric on the open four-ball). Another class of examples is provided by cohomogeneity one $SU(2)$ -invariant complete ESD metrics, which were classified in [15]. A distinguished subclass of the latter is provided by those metrics which admit an isometric $U(2)$ action. These are the Pedersen metrics on the open four-ball [24] and their analytic continuations [24, 15]. As it turns out, these are the metrics relevant for the counter-example of [9]³.

What will allow us to make progress is the recent work of Calderbank and Pedersen [10], which gave an explicit description of the most general ESD space admitting two commuting and linearly independent Killing vector fields. Through an elegant chain of arguments, they showed that such spaces are described by a single function F of two variables, which is constrained to obey a *linear* PDE (namely, F must be an eigenfunction of the two-dimensional hyperbolic Laplacian with eigenvalue $3/4$). An immediate consequence of this linear description is that one can obtain new solutions (at least locally) by superposing various eigenfunctions F — a situation which is quite unexpected at first sight.

For the case of *positive* scalar curvature, the work of [10] has another application: it leads to an elegant description of ESD metrics on certain compact toric orbifolds which include and generalize the models studied a while ago by Galicki and Lawson [16]. As explained in [18] and [19], this can be combined with the construction of [17] and [21] in order to produce a large class of conical G_2 metrics, which lead to interesting M-theory backgrounds which produce chiral field theories in four dimensions [20]. The main simplification for the positive curvature case is due to Myers's theorem, which forces such spaces to be compact (if complete); this makes them amenable to (hyperkähler) toric geometry techniques upon invoking the associated hyperkähler cone/Swann bundle. In particular, this allows one to extract *global* information by simple computations in integral linear algebra.

When studying hypermultiplets, the ESD space of interest has negative scalar curvature and the isometries of M may fail to be compact. Therefore, toric geometry techniques do not always apply. This reflects the well-known observation that the global study of Einstein manifolds of negative scalar curvature is considerably more involved than the positive curvature case. In particular, it is not trivial to find functions

³The authors of [9] use a parameterization due to [26], which is quite different from that of [10] and [24], and somewhat cumbersome for our purpose. The relation between their coordinates and those of [24] is described in Appendix A.

F for which the metric of [10] is smooth and complete as required by supergravity applications. A class of such solutions was recently given by Calderbank and Singer [22], and in this paper we shall restrict to negative curvature models of that type. The metrics of [22] are smooth and complete, and live on an open subset M_+ of a toric resolution M of an Abelian quotient singularity $\mathbf{C}^2/\mathbf{Z}_p$; the set M_+ contains all irreducible components of the exceptional divisor. To ensure negative scalar curvature, one must require $c_1(M) < 0^4$. These models admit two Killing vectors with *compact* orbits, and thus they are invariant under a $U(1)^2$ action. As pointed out in [10, 22], such models are a generalization of the Pedersen–LeBrun metrics [24, 25]; the latter arise as the particular case when $M = \mathcal{O}(-p) \rightarrow \mathbf{P}^1$ is the minimal resolution of $\mathbf{C}^2/\mathbf{Z}_p$ with the *symmetric* \mathbf{Z}_p action $(z_1, z_2) \rightarrow (e^{2\pi i/p} z_1, e^{2\pi i/p} z_2)$. As mentioned above, the Pedersen metrics are invariant with respect to a larger $U(2) = SU(2) \times U(1)$ action and fit into the cohomogeneity one classification of $SU(2)$ invariant ESD metrics given by Hitchin [15].

The main advantage of the metrics of [22] is that the underlying manifold admits a toric description, even though the metrics themselves have negative scalar curvature. Indeed, the resolution M is a (noncompact) toric variety in two complex dimensions, whose combinatorial description is a classical result [27, 29]. In particular, the orbits of the isometric T^2 action can be described by standard methods of toric geometry [28, 29, 30, 31]. When considering flows on such spaces, this allows for easy identification of the critical points of the relevant superpotential since, in the absence of vector/tensor multiplets, the latter are the fixed points of the $U(1)$ isometry used to gauge the supergravity action [12, 13].

In fact, the basic picture can be explained quite easily in non-technical language. Recall that the toric variety M can be presented as a T^2 -fibration over its Delzant polytope Δ_M^5 . In our case, the latter is a noncompact planar polytope and general results [29, 31] show that the T^2 fiber of M collapses to a point at its vertices and to a circle above its edges. The S^1 fibrations above the finite edges (whose circle fibers collapse to points at the vertices) give a collection of smooth spheres S_j which are holomorphically embedded in M — one obtains a copy of \mathbf{P}^1 for every finite edge of Δ_M . A generic isometry fixes only the points p_j of M sitting above the vertices of Δ_M . As one can obtain an arbitrary number of points p_j by taking p (M is the resolution of $\mathbf{C}^2/\mathbf{Z}_p$) to be large, *one can produce models with an arbitrarily large*

⁴Compare this with the Gorenstein case $c_1(M) = 0$ (A_{p-1} surface singularities), which leads to the well-known hyperkahler metrics of Eguchi–Hanson and Gibbons–Hawking [23].

⁵This fibration arises by considering the moment map $\mu : M \rightarrow \mathbf{R}^2$ of the $U(1)^2$ action with respect to the toric Kahler metric of M . The Delzant polytope Δ_M is the image $\mu(M) \subset \mathbf{R}^2$. Note that the toric Kahler metric of M differs from its ESD metric.

number of isolated critical points of the superpotential. This should be contrasted with the Pedersen metrics considered in [9], which lead to at most two isolated critical points. This observation will allow us to build chains of flows connecting the critical points, and therefore domain wall solutions which interpolate between the associated AdS_5 backgrounds.

For a general choice of gauged isometry, it turns out that at most one such flow is of Randall-Sundrum type (i.e it connects two IR critical points). Among the rest, there are domain wall solutions which interpolate between a UV and an IR critical point. Some of these may describe RG flows of appropriate dual field theories due to the following chain of arguments. It is believed that 5-dimensional $N = 8$ gauged supergravity [33, 34] is a consistent truncation of the 10-dimensional IIB supergravity on $AdS_5 \times S^5$ (some evidence for this was presented in [35, 36]). This means that every solution of the former is also a solution of the latter. Although there is no proof at present, this is strongly supported by similarity with two other cases: 4-dimensional $N = 8$ gauged supergravity, which is known [37] to be a consistent truncation of 11-dimensional supergravity on $AdS_4 \times S^7$, and 7-dimensional gauged supergravity, which was shown recently [38] to be a consistent truncation of 11-dimensional supergravity on $AdS_7 \times S^4$. Additional, indirect evidence for the consistency of the truncation of IIB SUGRA on $AdS_5 \times S^5$ to $d = 5$, $N = 8$ SUGRA is provided by the numerous studies in AdS/CFT (for example [39, 40]), where that consistency is assumed and domain walls of the supergravity theory are interpreted as RG flows of the corresponding dual field theory. Various quantities, calculated both from the gravity side and from the field theory side, have been successfully matched [39, 40]. For one of these solutions — a domain wall in 5d $N = 8$ supergravity, which describes an RG flow from $N = 4$ to $N = 1$ super Yang-Mills driven by the addition of a mass term for one of the three adjoint chiral superfields [39] — it was found in [12] that it can be embedded in 5d $N = 2$ gauged supergravity. In particular this means that the $N = 2$ theory is at least in that case a consistent truncation of the 10d IIB theory. This may be by chance, but it may also be that many more domain walls of 5d $N = 2$ SUGRA can be embedded in the 10d theory and hence can have via the AdS/CFT correspondence an interpretation as a RG flow of an appropriate field theory. It would be interesting to explore whether some of our UV-IR flows have such interpretations.

The present paper is organized as follows. In Section 2 we recall the necessary ingredients of 5-dimensional $N = 2$ gauged supergravity, and extract the superpotential and flow equations relevant for coupling the gravity multiplet to a single hypermultiplet described by the metric of [10]. Section 3 describes the subclass of metrics constructed in [22]. In Section 4 we study the general properties of BPS flows for such models. In particular, we give the general flow solutions connecting our critical points and describe

the conditions under which such a solution has Randall-Sundrum type (i.e. is an IR-IR flow). Section 5 illustrates this discussion with a few explicit examples, which include and generalize the solution of [9]. Appendix A gives the coordinate transformation relating the Pedersen metrics to the models discussed in [9].

2. Flow equations on toric one-hypermultiplet moduli spaces

Consider coupling a single hypermultiplet to the supergravity multiplet in five dimensions. As the theory contains only one gauge field (namely the graviphoton), one can gauge at most one isometry of the hypermultiplet moduli space. The general Lagrangian of gauged minimal supergravity in five dimensions was derived in [11]⁶. When no vector/tensor multiplets are present⁷, the scalar potential induced by the gauging takes the form [12]:

$$\mathcal{V} = -6W^2 + \frac{9}{2}g^{XY}\partial_X W\partial_Y W, \quad (2.1)$$

where g_{XY} is the hypermultiplet metric and the "superpotential" W is given by:

$$W = \sqrt{\frac{2}{3}P^r P^r} \quad , \quad r = 1, 2, 3. \quad (2.2)$$

Here $\{P^r\}_{r=1}^3$ is the triplet of prepotentials related to the Killing vector K^Y of the gauged isometry:

$$\mathcal{R}_{XY}^r K^Y = 2D_X P^r, \quad (2.3)$$

where $\{\mathcal{R}^r\}_{r=1}^3$ is the triplet of $\text{Sp}(1)$ curvatures and D_X is the full covariant derivative (including the Levi-Civita, $\text{Sp}(n)$ and $\text{Sp}(1)$ connections for the case of a $4n$ -dimensional quaternionic space). The factor of 2 is a result of a different normalization w.r.t. [12, 9] as will be explained below.

Note that we work with the convention [12] that W is always non-negative (i.e. we choose the non-negative square root in (2.2)). This implies that W will fail to be differentiable at a zero of W where the directional derivatives do not all vanish. At such a *noncritical zero*, the function W^2 is differentiable, and its Hessian is positive semidefinite [13].

In our example, we take $n = 1$ and let the hypermultiplet moduli space be described by a T^2 invariant ESD metric of negative scalar curvature. As shown in [10], the most general T^2 invariant ESD metric has the form:

$$d\sigma^2 = \frac{|F^2 - 4\rho^2(F_\rho^2 + F_\eta^2)|}{4F^2} \frac{d\rho^2 + d\eta^2}{\rho^2} + \frac{[(F - 2\rho F_\rho)\alpha - 2\rho F_\eta\beta]^2 + [-2\rho F_\eta\alpha + (F + 2\rho F_\rho)\beta]^2}{F^2|F^2 - 4\rho^2(F_\rho^2 + F_\eta^2)|} \quad (2.4)$$

⁶Minimal means $N = 2$ as in 5d there is no $N = 1$ gauged supergravity theory.

⁷When including vector/tensor multiplets, the potential can not always be written in this form. See [12] for details.

where $\alpha = \sqrt{\rho} d\phi$, $\beta = (d\psi + \eta d\phi)/\sqrt{\rho}$ and the function $F(\rho, \eta)$ satisfies the equation:

$$\rho^2(F_{\rho\rho} + F_{\eta\eta}) = \frac{3}{4}F. \quad (2.5)$$

Note that we use the notation $F_\rho = \partial_\rho F$, $F_\eta = \partial_\eta F$, $F_{\rho\rho} = \partial_\rho^2 F$ etc. for the partial derivatives of F .

In equation (2.4), one takes $\rho > 0$ and $\eta \in \mathbf{R}$, while ϕ, ψ are coordinates of periodicity 2π . The metric is well-defined for $F^2 \neq 4\rho^2(F_\rho^2 + F_\eta^2)$ and $F \neq 0$. It has positive scalar curvature in the regions where $F^2 - 4\rho^2(F_\rho^2 + F_\eta^2) > 0$ and negative scalar curvature for $F^2 - 4\rho^2(F_\rho^2 + F_\eta^2) < 0$. One can easily check that (2.4) is normalized so that in the latter case the scalar curvature is -12 as is usual for supergravity applications.

Condition (2.5) says that F is an eigenfunction (with eigenvalue $3/4$) of the hyperbolic Laplacian $\Delta_{\mathcal{H}} = \rho^2(\partial_\rho^2 + \partial_\eta^2)$. This is the Laplacian of the standard metric:

$$ds_{\mathcal{H}}^2 = \frac{1}{\rho^2}(d\rho^2 + d\eta^2) \quad (2.6)$$

on the hyperbolic plane \mathcal{H}^2 with coordinates $\rho > 0$ and $\eta \in \mathbf{R}$. Note that we use the upper half plane model.

The Sp(1) curvatures determined by (2.4) are [10]:

$$\begin{aligned} \mathcal{R}^1 &= -\frac{F^2 - 4\rho^2(F_\rho^2 + F_\eta^2)}{4F^2\rho^2} d\rho \wedge d\eta + \frac{1}{F^2} d\phi \wedge d\psi \\ \mathcal{R}^2 &= \frac{F_\eta}{F^2\sqrt{\rho}} d\psi \wedge d\rho + \frac{1}{F^2\sqrt{\rho}} \left(\rho F_\rho + \eta F_\eta - \frac{F}{2} \right) d\phi \wedge d\rho \\ &\quad - \frac{1}{F^2\sqrt{\rho}} \left(F_\rho + \frac{F}{2\rho} \right) d\psi \wedge d\eta + \frac{1}{F^2\sqrt{\rho}} \left(\rho F_\eta - \eta F_\rho - \frac{\eta F}{\rho} \right) d\phi \wedge d\eta \\ \mathcal{R}^3 &= -\frac{1}{F^2\sqrt{\rho}} \left(F_\rho + \frac{F}{2\rho} \right) d\psi \wedge d\rho + \frac{1}{F^2\sqrt{\rho}} \left(\rho F_\eta - \eta F_\rho - \frac{\eta F}{\rho} \right) d\phi \wedge d\rho \\ &\quad - \frac{F_\eta}{F^2\sqrt{\rho}} d\psi \wedge d\eta - \frac{1}{F^2\sqrt{\rho}} \left(\rho F_\rho + \eta F_\eta - \frac{F}{2} \right) d\phi \wedge d\eta. \end{aligned} \quad (2.7)$$

It is easy to check that they satisfy:

$$\mathcal{R}_{XY}^r \mathcal{R}^{sYZ} = -\delta^{rs} \delta_X^Z - \varepsilon^{rst} \mathcal{R}_X^t{}^Z \quad (2.8)$$

unlike (2.11) of [12]. Hence these curvatures are normalized to

$$\mathcal{R}_{XY}^r = -J_{XY}^r, \quad (2.9)$$

where J^r are the three complex structures, and not to $\mathcal{R}^r = -\frac{1}{2}J^r$ as in [12, 9]. With this normalization the covariant derivative takes the form

$$D_X P^r = \partial_X P^r + \varepsilon^{rst} \omega_X^s P^t \quad (2.10)$$

on a quantity having only an $\text{Sp}(1)$ index. Note the slight difference w.r.t. (2.12) of [12]. In (2.10) $\{\omega^s\}_{s=1}^3$ is the triplet of $\text{Sp}(1)$ connections for the curvature (2.7) [10]:

$$\omega^1 = -\frac{F_\eta}{F} d\rho + \left(\frac{1}{2\rho} + \frac{F_\rho}{F} \right) d\eta \quad , \quad \omega^2 = -\frac{\sqrt{\rho}}{F} d\phi \quad , \quad \omega^3 = \frac{\eta}{F\sqrt{\rho}} d\phi + \frac{1}{F\sqrt{\rho}} d\psi. \quad (2.11)$$

Using (2.8) one can solve (2.3) for the Killing vector:

$$K^Y = -\frac{2}{3} \mathcal{R}^{rYX} D_X P^r. \quad (2.12)$$

Again the numerical factor differs slightly from [12, 9] due to the different normalization of the $\text{Sp}(1)$ curvatures and connections. Equation (2.3) can also be solved for the prepotentials by using the fact that they are eigenfunctions of the Laplacian [14]:

$$D^X D_X P^r = -2n P^r \quad (2.13)$$

(for a $4n$ -dimensional quaternion-Kähler space). Again this differs by a factor of 2 w.r.t. the footnote after (2.15) in [12]. One obtains:

$$P^r = -\frac{1}{4} D_X (K^Z g_{ZY} \mathcal{R}^{rXY}) = -\frac{1}{4} \mathcal{R}^{rXY} \partial_X K_Y, \quad (2.14)$$

where the second equality results from the covariant constancy and antisymmetry in X and Y of the $\text{Sp}(1)$ curvature. A domain wall of gauged supergravity,

$$ds^2 = e^{2U(t)} dx_{4d}^2 + dt^2, \quad (2.15)$$

which preserves $N = 1$ supersymmetry is given by the solution of the following system [12]:

$$\begin{aligned} \partial_t U &= \pm g W \\ \partial_t q^X &= \mp 3g g^{XY} \partial_Y W, \end{aligned} \quad (2.16)$$

where q^X are the hypermultiplet scalars. The signs in these equations must be chosen consistently (i.e. one must use the minus sign in the second equation if one chooses the plus sign in the first). In order to insure continuity of the derivative of a flow which passes through a noncritical zero of W , one must switch the sign in the first equation

when the flow meets such a point. Accordingly, the sign in the second equation must also be switched there.

Let us gauge the isometry of the metric (2.4) along the Killing vector:

$$K = \partial_\phi - \lambda \partial_\psi. \quad (2.17)$$

Note that we normalize K such that the coefficient of its ∂_ϕ component equals one.

Observation Equation (2.3) fixes the prepotentials P^r (and thus the superpotential (2.2)) in terms of a specific choice for the Killing vector K . In particular, rescaling K leads to a rescaling of W , which can be absorbed by a rescaling of t in equations (2.16). Since the first of these equations determines U only up to a constant factor, this rescaling of t can be further absorbed into a constant rescaling of the metric (2.15), upon choosing an appropriate integration constant for U . In particular, the normalization in (2.17) amounts to a particular choice of scale for t or, equivalently, a choice of scale for the metric (2.15).

Equation (2.14) implies:

$$P^1 = 0, \quad P^2 = \frac{1}{2} \frac{\sqrt{\rho}}{F}, \quad P^3 = -\frac{1}{2} \frac{\eta - \lambda}{F \sqrt{\rho}} \quad (2.18)$$

where we took (2.5) into account. Using (2.12), one can check that these prepotentials give (2.17). Now (2.2) gives:

$$W = \sqrt{\frac{1}{6F^2} \left[\rho + \frac{(\eta - \lambda)^2}{\rho} \right]}. \quad (2.19)$$

Because W is only a function of ρ and η and the metric (2.4) (and hence its inverse) is diagonal in ρ, η , the potential (2.1) and the "flow equations" (2.16) acquire a particularly simple form:

$$\mathcal{V} = -\frac{1}{F^2} \left(\rho + \frac{(\eta - \lambda)^2}{\rho} \right) + \frac{18\rho^2 F^2}{|F^2 - 4\rho^2(F_\rho^2 + F_\eta^2)|} [(\partial_\rho W)^2 + (\partial_\eta W)^2], \quad (2.20)$$

and:

$$\begin{aligned} \frac{d\phi}{dt} &= \frac{d\psi}{dt} = 0 \\ \frac{dU}{dt} &= \pm gW \end{aligned}$$

$$\begin{aligned}\frac{d\rho}{dt} &= \mp 12g \frac{\rho^2 F^2}{|F^2 - 4\rho^2(F_\rho^2 + F_\eta^2)|} \partial_\rho W \\ \frac{d\eta}{dt} &= \mp 12g \frac{\rho^2 F^2}{|F^2 - 4\rho^2(F_\rho^2 + F_\eta^2)|} \partial_\eta W.\end{aligned}\tag{2.21}$$

Hence the T^2 isometry of the one-hypermultiplet moduli space allows us to reduce the four-dimensional flow equations to a two-dimensional problem. The last two relations describe the gradient flow of W with respect to the metric $\frac{|F^2 - 4\rho^2(F_\rho^2 + F_\eta^2)|}{\rho^2 F^2} (d\rho^2 + d\eta^2)$ on the upper half plane (notice that this is conformal to the hyperbolic metric).

3. Calderbank-Singer spaces

3.1 Minimal resolutions of cyclic quotient singularities

Consider a cyclic singularity $\mathbf{C}^2/\mathbf{Z}_p$, where the generator of \mathbf{Z}_p acts through:

$$(z_1, z_2) \rightarrow (e^{2\pi i/p} z_1, e^{2\pi i q/p} z_2) .\tag{3.1}$$

We assume that the integers p, q satisfy $p > q > 0^8$. We consider the *minimal* resolution of this singularity, which is a smooth algebraic surface M birational with $\mathbf{C}^2/\mathbf{Z}_p$ and containing no -1 curves. If $S_1 \dots S_k$ denote the irreducible components of its exceptional divisor, then it is a classical fact [27] that the intersection matrix of these components has the form:

$$(S_i \cdot S_j) = \begin{bmatrix} -e_1 & 1 & 0 & \dots & 0 \\ 1 & -e_2 & 1 & \dots & 0 \\ 0 & 1 & -e_3 & \dots & 0 \\ \dots & \dots & \dots & \dots & \dots \\ 0 & 0 & 0 & \dots & -e_k \end{bmatrix} ,\tag{3.2}$$

where the diagonal entries are integers satisfying $e_j \geq 2$. The adjunction formula shows that $c_1(M) \leq 0$, with $c_1(M) < 0$ if and only if all $e_j \geq 3$ and $c_1(M) = 0$ iff all $e_j = 2$;

⁸This action embeds diagonally in $U(2)$. It embeds in $SU(2)$ if and only if $q + 1 = p$, when the singularity $\mathbf{C}^2/\mathbf{Z}_p$ is called *Gorenstein* and has trivial dualizing sheaf; in that case, it is simply an A_{p-1} surface singularity. In this paper, we are emphatically *not* interested in the Gorenstein case. We note that non-Gorenstein cyclic singularities arise naturally in the study of normal complex surfaces—this generalizes the better known case of A_{p-1} singularities, which give local descriptions for the singularities of $K3$. The minimal resolution of an A_{p-1} singularity has trivial first Chern class and carries the multi-Eguchi-Hanson metric, which is hyperkahler. As shown in [22], such resolutions *never* carry a toric SDE metric of negative scalar curvature.

the latter case corresponds to $q = p - 1$ (the A_{p-1} Gorenstein singularity). For what follows, we shall consider exclusively the case $c_1(M) < 0$.

It is well known that both $\mathbf{C}^2/\mathbf{Z}_p$ and its minimal resolution are toric varieties (see, for example, [29]). As explained in [29], the toric description of X can be extracted with the help of continued fractions. Indeed the integers k and $e_1 \dots e_k$ are given by the *minus*⁹ continued fraction expansion:

$$\frac{p}{q} = e_1 - \frac{1}{e_2 - \frac{1}{e_3 - \dots - \frac{1}{e_{k-1} - \frac{1}{e_k}}}} \quad , \quad (3.3)$$

which we shall denote by $(e_1 \dots e_k)$ for simplicity. The toric data of M can be determined as follows [29]¹⁰. Consider a basis (t, t') of the two-dimensional lattice \mathbf{Z}^2 , and define vectors $\nu_0 \dots \nu_k$ by the two-step recursion:

$$\nu_{j+1} = e_j \nu_j - \nu_{j-1} \quad (j = 1 \dots k) \quad , \quad (3.4)$$

with the initial conditions $\nu_0 = t$ and $\nu_1 = t + t'$. Then $\nu_{k+1} = (p - q)t + pt'$ and $\nu_0 \dots \nu_{k+1}$ are the toric generators of the minimal resolution M , while ν_0 and ν_{k+1} are the toric generators of the singularity $\mathbf{C}^2/\mathbf{Z}_p$. The latter generate a (strongly convex) cone σ , subdivided by the vectors $\nu_1 \dots \nu_k$ which lie in its interior. In fact, these vectors coincide with the vertices of the convex polytope defined by the convex hull of the intersection of $\sigma - \{0\}$ with the \mathbf{Z}^2 lattice. Following [22], we choose $t = \begin{bmatrix} 0 \\ -1 \end{bmatrix}$

and $t' = \begin{bmatrix} 1 \\ 1 \end{bmatrix}$ (always possible via a modular transformation), which gives $\nu_0 = \begin{bmatrix} 0 \\ -1 \end{bmatrix}$,

$\nu_1 = \begin{bmatrix} 1 \\ 0 \end{bmatrix}$ and $\nu_{k+1} = \begin{bmatrix} p \\ q \end{bmatrix}$. Upon writing $\nu_j = \begin{bmatrix} m_j \\ n_j \end{bmatrix}$, relation (3.4) becomes:

$$m_{j+1} = e_j m_j - m_{j-1} \quad , \quad n_{j+1} = e_j n_j - n_{j-1} \quad (j \geq 1) \quad , \quad (3.5)$$

with the initial conditions $(m_0, n_0) = (0, -1)$ and $(m_1, n_1) = (1, 0)$. These can be recognized as the standard recursion relations for the numerator and denominator of the partial quotients $q_j = (e_1 \dots e_j) = m_{j+1}/n_{j+1}$ ($j = 1 \dots k$) of the continued fraction (3.3). We remind the reader that the solutions of this recursion have the following properties (all of which can be checked by direct computation or induction):

⁹This differs from the more common ‘plus’ continued fractions. By definition of the expansion (3.3), the integers e_j are required to satisfy $e_j \geq 2$.

¹⁰Our presentation differs from that of [29] in a few trivial ways. First, reference [29] uses a different description of the cyclic action, which amounts to the redefinitions $p \rightarrow q$ and $q \rightarrow q - p$. It also writes our second order recursion as a first order recursion for two vectors.

(a) $n_0 = -1 < n_1 = 0 < n_2 = 1 < n_3 < \dots < n_{k+1} = q$ and $m_0 = 0 < m_1 = 1 < m_2 = e_1 < \dots < m_{k+1} = p$

(b) $q_1 > q_2 > \dots > q_k = p/q$.

(c) $m_j n_{j+1} - m_{j+1} n_j = 1$ for $j = 0 \dots k$ and $m_{j-1} n_{j+1} - m_{j+1} n_{j-1} = e_j$ for $j = 1 \dots k$.

(d) If all e_j are strictly greater than two, then $m_{j+1} - m_j > m_j - m_{j-1}$ for all $j = 1 \dots k$ and $n_{j+1} - n_j > n_j - n_{j-1}$ for all $j = 2 \dots k$.

The first part of (c) says that the area of the triangle determined by vectors ν_j and ν_{j+1} equals $1/2$ — this is the condition that the subdivision of the cone σ resolves the singularities of $\mathbf{C}^2/\mathbf{Z}_p$.

The situation for the vectors $\nu_0 \dots \nu_{k+1}$ is illustrated in figure 1. It shows the case $p = 8$ and $q = 3$, which will be discussed in more detail in Subsection 5.3.

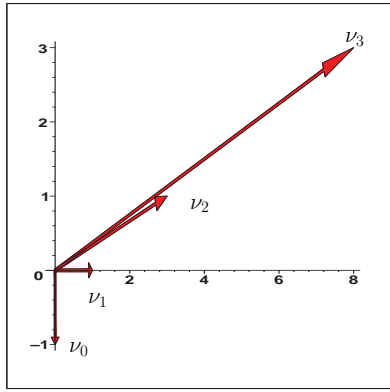


Figure 1: Toric generators for the model $(p, q) = (8, 3)$. In this case, one has $k = 2$.

3.2 The Calderbank-Singer metrics

In [22], Calderbank and Singer construct toric ESD metrics of negative scalar curvature on the minimal¹¹ resolutions of cyclic singularities with negative first Chern class. These metrics are invariant with respect to the natural T^2 action on M induced by its structure of toric variety. In view of the results of [10], they must have the general form (2.4) with $F^2 < 4\rho^2(F_\rho^2 + F_\eta^2)$, where the angular coordinates (ϕ, ψ) parameterize the T^2 fibers of M . This is achieved by choosing F to be a superposition of *elementary eigenfunctions*

¹¹In fact, the construction of [22] applies to a more general class of toric resolutions of $\mathbf{C}^2/\mathbf{Z}_p$, which are not necessarily minimal. In this paper, we shall consider their construction only for the case of minimal resolutions.

of the type:

$$f(\rho, \eta; y) = \sqrt{\rho + \frac{(\eta - y)^2}{\rho}} \quad , \quad (3.6)$$

which are easily seen to satisfy $\Delta_{\mathcal{H}} f = \frac{3}{4}f$. More precisely, one must choose the linear combination:

$$F(\rho, \eta) = \sum_{j=0}^{k+1} w_j f(\rho, \eta; y_j) \quad , \quad (3.7)$$

where:

$$w_j = \frac{1}{2}(m_j - m_{j+1}) \quad , \quad y_j = \frac{n_{j+1} - n_j}{m_{j+1} - m_j} \quad (3.8)$$

and we defined $m_{k+2} = 0$ and $n_{k+2} = 1$ (addition of $\nu_{k+2} := \begin{bmatrix} m_{k+2} \\ n_{k+2} \end{bmatrix}$ and thus of y_{k+1} amounts to taking the one-point compactification \overline{M} of M). Since we assume $c_1(M) < 0$, we have $e_j \geq 3$ for all $j = 1 \dots k$ and thus $w_{k+1} = p/2 > 0 > w_0 = -1/2 > w_1 > \dots > w_k$. The combination (3.7) is fixed (up to a constant scale factor) by the requirement that the metric (2.4) extends smoothly to the singular fibers of M . When considering the metric (2.4), one identifies topologically the boundary of the Delzant polytope Δ_M with the boundary $\rho = 0$ of the upper half plane model of the hyperbolic plane. Then the vertices of the Delzant polytope are mapped to the points $y_0 \dots y_k$, and its edges correspond to the intervals determined by these vertices. It is easy to check [22] that $y_0 > y_1 > \dots > y_k > q/p > y_{k+1}$, so that the edges of Δ_M correspond to the intervals $I_j := (y_j, y_{j-1})$ sitting at $\rho = 0$.

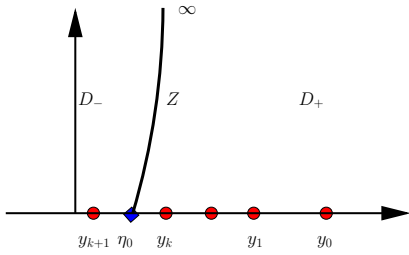


Figure 2: General arrangement of y_j , Z and $\eta_0 = q/p$ in the hyperbolic plane. The simple curve Z separates the upper half plane into the regions D_- and D_+ . The latter is the region of interest for the present paper.

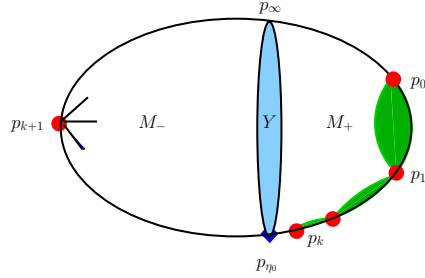


Figure 3: The open sets M_+ and M_- are separated by the conformal infinity Y . Each region M_{\pm} carries an ESD metric of negative scalar curvature. The point p_{k+1} (which lies above y_{k+1}) is an orbifold point; it is the ‘point at infinity’ of \overline{M} . The figure also shows the irreducible components of the exceptional divisor, which connect the points $p_0 \dots p_k$ lying above $y_0 \dots y_k$.

Expression (2.4) determines an ESD metric (of negative scalar curvature) on the space $\overline{M} \rightarrow \overline{\mathcal{H}}^2$, where $\overline{\mathcal{H}}^2$ is the conformal compactification of the hyperbolic plane (obtained by adding the point at infinity). However, this metric is ill-defined along the set Z given by the equation $F(\rho, \eta) = 0$. As explained in [22], this locus is a smooth simple curve which intersects the boundary of $\overline{\mathcal{H}}^2$ in the points $\eta_0 = q/p = 1/q_k \in (y_{k+1}, y_k)$ and ∞ (see figure 2). This curve separates $\overline{\mathcal{H}}^2$ into connected components D_+ (defined by the condition $F(\rho, \eta) > 0$) and D_- (defined by $F(\rho, \eta) < 0$), which pull back to two disjoint open subsets M_+ and M_- of \overline{M} , separated by a region Y defined as the pull-back of Z . The piece D_+ contains the points $y_0 \dots y_k$, while D_- contains the point y_{k+1} . The set Y is a compact T^2 fibration over Z , which coincides topologically with the Lens space S^3/\mathbf{Z}_p . It is a conformal infinity for each of the two ESD metrics determined by (2.4) on the open sets M_+ and M_- [10]. Note that M_+ contains the exceptional divisor of the resolution, and that the ESD metric induced on M_+ is smooth and complete. The metric induced on M_- is a complete orbifold metric, with the orbifold point given by the point at infinity of \overline{M} , which we denote by p_{k+1} (this point sits above y_{k+1}). Since we are interested in smooth and complete metrics, we shall concentrate on the region M_+ (see figure 3).

3.3 Fixed points of $U(1)$ isometries

The fibration of M over its Delzant polytope translates into a fibration over \mathcal{H}^2 . Since the points y_j correspond to the vertices of Δ_M , the T^2 fibers collapse to points above y_j and to circles above the intervals $I_j = (y_j, y_{j-1})$ sitting at $\rho = 0$. In expression (2.4), one uses coordinates (ϕ, ψ) along the T^2 fibers such that the vectors $\partial_\psi, \partial_\phi$ correspond to the canonical basis of the lattice \mathbf{Z}^2 . Hence the $U(1)$ generator (2.17) corresponds to the two-vector $\tau = \begin{bmatrix} -\lambda \\ 1 \end{bmatrix}$. This isometry fixes the sphere S_j lying above I_j precisely when τ is orthogonal to the generator ν_j , i.e. when $\lambda = \lambda_j := \nu_j^2/\nu_j^1 = n_j/m_j = 1/q_{j-1}$. Note that all isometries (2.17) fix the points p_j of M lying above y_j .

4. Supersymmetric flows on Calderbank-Singer spaces

4.1 Critical points of the superpotential

When the supergravity multiplet is coupled only to hypermultiplets but not to vector/tensor multiplets, it was shown in [12] and [13] that the critical points of the superpotential (2.19) coincide with the fixed points of the associated isometry (2.17). In view of the discussion above, we find that an isometry of M_+ with λ different from $\lambda_1 \dots \lambda_k$ fixes exactly the points $p_0 \dots p_k$; thus a generic isometry has $k + 1$ critical

points. In the non-generic cases $\lambda = \lambda_j$, the isometry fixes $p_0 \dots p_k$ together with the entire sphere S_j .

4.2 Asymptotic form of the flow equations and divisorial flows

The superpotential (2.19) can be written:

$$W = \frac{1}{\sqrt{6}} \frac{f(\rho, \eta, \lambda)}{F(\rho, \eta)} , \quad (4.1)$$

where we used $F > 0$ on the domain of interest D_+ . Let us write the flow equations (2.21) as:

$$\begin{aligned} \frac{dU}{dt} &= \pm g W \\ \frac{d\rho}{dt} &= \pm h(\rho, \eta) \\ \frac{d\eta}{dt} &= \mp g(\rho, \eta) , \end{aligned} \quad (4.2)$$

where:

$$\begin{aligned} h(\rho, \eta) &= 12g \frac{\rho^2 F^2}{F^2 - 4\rho^2(F_\rho^2 + F_\eta^2)} \partial_\rho W \\ g(\rho, \eta) &= -12g \frac{\rho^2 F^2}{F^2 - 4\rho^2(F_\rho^2 + F_\eta^2)} \partial_\eta W . \end{aligned} \quad (4.3)$$

It is not very hard to check the following asymptotics for h, g as $\rho \rightarrow 0$:

$$\begin{aligned} h(\rho, \eta) &= g \sqrt{\frac{3}{2}} \frac{\Phi - (\eta - \lambda)^2 \Theta}{(\Xi^2 - \Phi \Theta) |\eta - \lambda|} \rho + O(\rho^2) \\ g(\rho, \eta) &= g \sqrt{\frac{3}{2}} \frac{(\Phi - (\eta - \lambda) \Xi) \text{sign}(\eta - \lambda)}{\Xi^2 - \Phi \Theta} + O(\rho) . \end{aligned} \quad (4.4)$$

To arrive at these expressions, we defined:

$$\begin{aligned} \Phi(\eta) &= \sum_{j=0}^{k+1} w_j |\eta - y_j| \\ \Xi(\eta) &= \sum_{j=0}^{k+1} w_j \text{sign}(\eta - y_j) \\ \Theta(\eta) &= \sum_{j=0}^{k+1} \frac{w_j}{|\eta - y_j|} . \end{aligned} \quad (4.5)$$

In particular, one has $\lim_{\rho \rightarrow 0^+} h(\rho, \eta) = 0$, so that the gradient lines of W become orthogonal to the real axis for $\rho \rightarrow 0$. Thus one can find a flow (integral curve) along this axis by setting $\rho = 0$ consistently in equations (4.2). In this case, the second equation in (4.2) is trivially satisfied and the system reduces to:

$$\begin{aligned} \frac{dU}{dt} &= \pm gW(0, \eta) \\ \frac{d\eta}{dt} &= \mp g_0(\eta) \quad , \end{aligned} \quad (4.6)$$

where:

$$g_0(\eta) = \lim_{\rho \rightarrow 0^+} g(\rho, \eta) = g \sqrt{\frac{3}{2}} \frac{[\Phi - (\eta - \lambda)\Xi] \text{sign}(\eta - \lambda)}{\Xi^2 - \Phi\Theta} \quad . \quad (4.7)$$

Up to the factor $\mp 3g$, the second equation in (4.6) describes the one-dimensional gradient flow of the function:

$$W_0(\eta) := \lim_{\rho \rightarrow 0^+} W(\rho, \eta) = \frac{1}{\sqrt{6}} \frac{|\eta - \lambda|}{\Phi(\eta)} \quad (4.8)$$

with respect to the limiting metric:

$$g_{\eta\eta}^{(0)} = \lim_{\rho \rightarrow 0^+} g_{\eta\eta} = \frac{\Xi^2 - \Phi\Theta}{\Phi^2} \quad . \quad (4.9)$$

This induced metric blows up on the interval (η_0, ∞) precisely at the points $\eta = y_j$ ($j = 0 \dots k$), but this is a coordinate singularity. Note that (4.9) is continuous on $(\eta_0, \infty) - \{y_0 \dots y_k\}$. It is also clear¹² that the length of each interval (y_j, y_{j-1}) is finite with respect to this metric for $j = 1 \dots k$. The intervals (η_0, y_k) and $(y_0, +\infty)$ have infinite length since they bound the conformal infinity Z .

Since the region of M sitting above each interval $I_j := (y_j, y_{j-1})$ ($j = 1 \dots k$) is the 2-sphere S_j (a component of the exceptional divisor), it is clear that flows of type (4.6) lift to flows in M_+ which are entirely contained inside some S_j . The intersection matrix (3.2) shows that the dual graph of $S_1 \dots S_k$ is a chain, so S_j touches only S_{j-1} and S_{j+1} for $j = 2 \dots k-1$. Let χ_j be a coordinate along the uncollapsed circle above I_j . Since W and the metric (2.4) are independent of the fiber coordinates, the flow equations (2.16) require $\chi_j = \text{const}$ (this can also be seen from equations (2.21), since χ_j are certain linear combinations of the angular coordinates ϕ, ψ). Hence the flow

¹²This can be checked directly by noticing that $\sqrt{g_{\eta\eta}^{(0)}}$ blows up like $|\eta - y_j|^{-1/2}$ for $\eta \rightarrow y_j$. Hence the distance $\int_{y_j}^{y_{j-1}} \sqrt{g_{\eta\eta}^{(0)}} d\eta$ stays finite. It also follows from the fact that the metric of [22] is adapted to the toric fibration $M \rightarrow \Delta_M$, which restricts to the two-sphere S_j over each interval I_j .

proceeds along the sphere S_j at some fixed angular value χ_j (figure 4). Since such flows are restricted to lie in the exceptional divisor, we shall call them *divisorial flows*.

As explained after relations (2.16), the sign in equations (4.6) must be switched when the flow passes through a noncritical zero of W . This means that the divisorial flow equations can be written in the form:

$$\begin{aligned} \frac{dU}{dt} &= -\epsilon g W_c \\ \frac{d\eta}{dt} &= \epsilon g_c(\eta) \quad , \end{aligned} \quad (4.10)$$

where:

$$W_c(\eta) := \frac{1}{\sqrt{6}} \frac{\eta - \lambda}{\Phi(\eta)} \quad (4.11)$$

and:

$$g_c(\eta) = g \sqrt{\frac{3}{2} \frac{\Phi - (\eta - \lambda)\Xi}{\Xi^2 - \Phi\Theta}} \quad , \quad (4.12)$$

where $\epsilon \in \{-1, 1\}$ is now *constant* along each given flow ¹³.

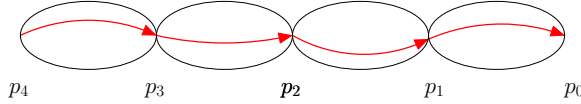


Figure 4: Picture of divisorial flows for the case $k = 4$.

4.3 General properties of divisorial flows

To understand the general properties of the flow (4.10), we must analyze the quantities Φ , Ψ and Ξ . Notice that the first function can be written in the form [22]:

$$\Phi(\eta) = m_j \eta - n_j \quad \text{for } \eta \in I_j = (y_j, y_{j-1}) \quad . \quad (4.13)$$

Using this observation, it is easy to see that Φ has exactly one zero, namely $\eta = \eta_0 = q/p$ (the point where Z meets the axis $\rho = 0$, see figure 5). Moreover, Φ is strictly greater than zero for $\eta > \eta_0$ (the boundary of the domain of interest D_+) and smaller than zero for $\eta < \eta_0$ (the boundary of the complementary domain D_-). (In fact, Φ coincides with the limit $\lim_{\rho \rightarrow 0^+} \sqrt{\rho} F$). In particular, the point η_0 is a conformal infinity for the one-dimensional metric (4.9), as expected from the fact that the latter is the restriction of (2.4) to the real axis. Since we are interested in the domain D_+ , we shall restrict to $\eta > \eta_0$ in what follows.

¹³For the examples of Section 5, we shall take all divisorial flows to have $\epsilon = +1$.

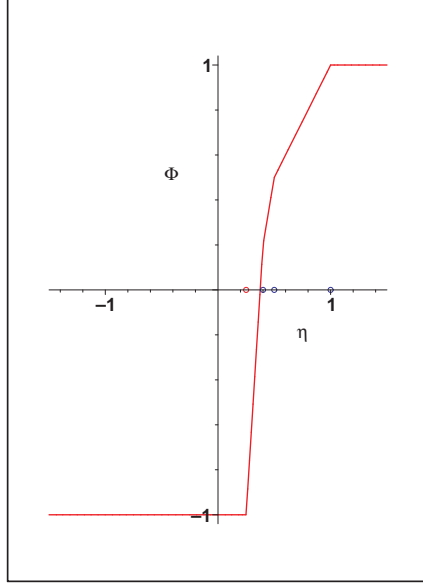


Figure 5: The function Φ for the model $(p, q) = (8, 3)$.

Expression (4.8) shows that $W_0(\eta)$ has a zero at $\eta = \lambda$, which will belong to the region of interest only when $\lambda > \eta_0$. Notice that:

$$\frac{dW_0}{d\eta} = -|\eta - \lambda| \frac{\Xi}{\Phi^2} + \frac{\text{sign}(\eta - \lambda)}{\Phi} \quad \text{for } \eta > \eta_0 \quad , \quad (4.14)$$

where we used the relation $\frac{d\Phi}{d\eta} = \Xi$. While this quantity does not vanish at $\eta = \eta_j$, the gradient field (4.7) does vanish there because Θ (and thus $g_{\eta\eta}^{(0)}$ given in (4.9)) blows up at these points. Once again, this is a peculiarity of our coordinate system. It is clear from (4.14) that the derivative of W_0 is discontinuous at y_j . The same is true for the gradient field $g_0(\eta)$. Taking $\eta \in I_j := (y_j, y_{j-1})$, we obtain:

$$W_0(\eta) = \frac{1}{m_j \sqrt{6}} \frac{|\eta - \lambda|}{\eta - \lambda_j} = \frac{\text{sign}(\eta - \lambda)}{m_j \sqrt{6}} \left[1 - \frac{\lambda - \lambda_j}{\eta - \lambda_j} \right] \quad \text{for } \eta \in I_j \quad . \quad (4.15)$$

(remember that $\lambda_j = n_j/m_j$ is the value of λ corresponding to the isometry which fixes S_j). By property (b) of Subsection 3.1, we have $\eta_0 = 1/q_k > 1/q_{j-1} = \lambda_j$, so that $\eta - \lambda_j > 0$ for $\eta > \eta_0$. Thus W is constant on (y_j, y_{j-1}) if $\lambda = \lambda_j$, in agreement with the fact that the isometry defined by this value of λ fixes the locus S_j . Since $\lambda_j < y_j$, we find that W_0 is nonsingular (and non-negative) along this interval. It will be monotonous on the entire interval unless $\lambda \in (y_j, y_{j-1})$, in which case it decreases for $\eta \in (y_j, \lambda)$ and increases for $\eta \in (\lambda, y_{j-1})$ (since $\lambda - \lambda_j > 0$). It is also clear that

the sign-corrected superpotential (4.11) is always monotonous on I_j and will be strictly increasing if $\lambda \in I_j$:

$$W_c(\eta) = \frac{1}{m_j \sqrt{6}} \left(1 - \frac{\lambda - \lambda_j}{\eta - \lambda_j} \right) \quad \text{for } \eta \in I_j \quad . \quad (4.16)$$

Finally, note that the sign-corrected gradient field (4.12) is continuous along I_j for all values of λ .

Equations (4.10) can be integrated by quadratures on each interval I_j . In fact, it is possible to obtain the general form of the solution of the second equation along such an interval. To find it, let us assume that $\eta \in I_j$. Then it is easy to check that $\Xi(\eta) = m_j$. Combining this with $\Phi(\eta) = m_j \eta - n_j$ allows us to compute:

$$\begin{aligned} \Xi^2 - \Phi\Theta &= m_j^2 - m_j(\eta - \lambda_j) \sum_{i=0}^{k+1} \frac{w_i}{|\eta - y_i|} \\ \Phi - (\eta - \lambda)\Xi &= \lambda m_j - n_j \quad , \end{aligned} \quad (4.17)$$

where we used $\lambda_j = n_j/m_j$. To simplify the first expression, write $|\eta - y_i| = \epsilon_{ij}(\eta - y_i)$, where $\epsilon_{ij} = \text{sign}(\eta - y_i)$ equals $+1$ for $i \geq j$ and -1 otherwise. Using $\frac{\eta - \lambda_j}{\eta - y_i} = 1 + \frac{y_i - \lambda_j}{\eta - y_i}$, we obtain:

$$\Xi^2 - \Phi\Theta = -m_j \sum_{i=0}^{k+1} \epsilon_{ij} \frac{w_i(y_i - \lambda_j)}{\eta - y_i} \quad , \quad (4.18)$$

where we used $\sum_{i=0}^{k+1} w_j \epsilon_{ij} = \sum_{i=0}^{k+1} w_j \text{sign}(\eta - y_i) = \Xi = m_j$.

This allows us to write the sign-corrected gradient in the form:

$$g_c(\eta) = -g \sqrt{\frac{3}{2}} \frac{\lambda - \lambda_j}{\sum_{i=0}^{k+1} \epsilon_{ij} \frac{w_i(y_i - \lambda_j)}{\eta - y_i}} \quad . \quad (4.19)$$

The second equation in (4.10) now integrates to:

$$\int d\eta \frac{1}{g_c(\eta)} = \epsilon t \quad , \quad (4.20)$$

with

$$\int d\eta \frac{1}{g_c(\eta)} = -\frac{1}{g(\lambda - \lambda_j)} \sqrt{\frac{2}{3}} \sum_{i=0}^{k+1} \epsilon_{ij} w_i (y_i - \lambda_j) \ln |\eta - y_i| + \text{constant} \quad . \quad (4.21)$$

Equation (4.20) gives the implicit form of the solution $\eta(t)$ on the interval I_j :

$$\sum_{i=0}^{k+1} \epsilon_{ij} w_i (y_i - \lambda_j) \ln |\eta - y_i| = -g \sqrt{\frac{3}{2}} (\lambda - \lambda_j) \epsilon t \quad . \quad (4.22)$$

To arrive at this relation, we used the freedom of performing a flow re-parameterization $t \rightarrow t + \text{constant}$ in order to absorb the additive constant of integration ¹⁴ (this re-parameterization does not affect the behavior of the flow for $t \rightarrow \pm\infty$).

To understand the behavior of (4.22) near the endpoints of I_j , let us compute:

$$\begin{aligned}\epsilon_{jj}w_i(y_j - \lambda_j) \ln |\eta - y_j| &= -\frac{1}{2m_j} \ln |\eta - y_j| \\ \epsilon_{j-1,j}w_i(y_{j-1} - \lambda_j) \ln |\eta - y_{j-1}| &= +\frac{1}{2m_j} \ln |\eta - y_j| \quad ,\end{aligned}\tag{4.23}$$

where we used the first relations in (c) of Subsection 3.1. Since $\ln(0^+) = -\infty$, this shows that η tends to y_j for $\epsilon(\lambda - \lambda_j)t \rightarrow -\infty$ and to y_{j-1} for $\epsilon(\lambda - \lambda_j)t \rightarrow +\infty$. Thus the flow starts at one end of I_j at $t = -\infty$ and reaches the other end at $t = +\infty$.

4.4 Flows of Randall-Sundrum type

Recall that a flow is of Randall-Sundrum [5] type if it connects two ‘IR critical points’ of W , i.e. two critical points for which the Hessian of W is negative semidefinite [32]. A divisorial flow along I_j will be of this type if and only if W_0 attains local maxima at the endpoints y_j, y_{j-1} of the flow. This condition requires that the flow pass through a zero of W . In view of the discussion above, this happens if and only if the flow parameter λ belongs to the interval I_j . Fixing $\lambda \in (y_k, y_0) - \{y_1 \dots y_{k-1}\}$, one finds a unique interval I_j ($j = 1 \dots k$) containing λ . The flow along this interval is of Randall-Sundrum type, while flows along the remaining intervals connect UV to UV or UV to IR fixed points (figure 6). In particular, this proves the existence of Randall-Sundrum flows (for a certain range of λ) for every model in our family. We also note that flows with $\eta > y_0$ or $\eta < y_k$ will necessarily extend to the conformal infinity Z , since W grows to infinity there. Such unbounded flows correspond to domain walls which connect a degenerate solution (associated with the conformal infinity) with one of the UV/IR AdS_5 solutions defined by the critical points y_0 and y_k . An unbounded flow of this type will pass through a zero of W if $\lambda \in (\eta_0, y_0)$ or $\lambda \in (y_k, +\infty)$ respectively. For the remainder of this paper we shall concentrate on divisorial flows, which proceed along one of the finite intervals I_j .

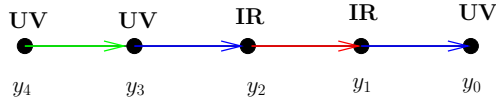


Figure 6: Schematic depiction of divisorial flows for $\lambda \in (y_2, y_1)$ (without considering the angular variables χ_j along the two-spheres). The figure shows the case $k = 4$.

¹⁴A similar re-parameterization can be used to clear the denominators in the logarithms of (4.22), an observation which will be used repeatedly in the examples of Section 5.

If $\lambda \in I_j = (y_j, y_{j-1})$, then the values of the superpotential at the endpoints of this interval are given by (4.15):

$$W_0(y_j) = \frac{1}{m_j \sqrt{6}} \frac{|y_j - \lambda|}{\eta - \lambda_j}, \quad W_0(y_{j-1}) = \frac{1}{m_j \sqrt{6}} \frac{|y_{j-1} - \lambda|}{\eta - \lambda_j}. \quad (4.24)$$

Requiring $W_0(y_j) = W_0(y_{j-1})$ with $\lambda \in I_j$ gives $\lambda = \frac{y_j + \alpha_j y_{j-1}}{1 + \alpha_j}$, where $\alpha_j := \frac{y_j - \lambda_j}{y_{j-1} - \lambda_j}$. Using property (c) of Subsection 3.1, we obtain $\alpha_j = \frac{m_j - m_{j-1}}{m_{j+1} - m_j}$, which leads to the following expression for λ :

$$\lambda = \frac{n_{j+1} - n_{j-1}}{m_{j+1} - m_{j-1}} := \lambda^{(j)}. \quad (4.25)$$

Thus we can always choose λ such that W has equal values at the endpoints of a Randall-Sundrum flow. With this choice of flow parameter, we obtain:

$$W_0(y_j) = W_0(y_{j-1}) = \frac{1}{\sqrt{6}} \frac{e_j - 2}{m_{j+1} - m_{j-1}}, \quad (4.26)$$

where we used property (c) of Subsection 3.1. We also note that $\lambda^{(j)} - \lambda_j = \frac{2}{m_j(m_{j+1} - m_{j-1})} > 0$, so that a Randall-Sundrum flow will satisfy:

$$\begin{aligned} \eta(t) &\rightarrow y_j && \text{for } \epsilon t \rightarrow -\infty \\ \eta(t) &\rightarrow y_{j-1} && \text{for } \epsilon t \rightarrow +\infty. \end{aligned} \quad (4.27)$$

In particular, η flows from the lower to the upper end of I_j if one takes $\epsilon = +1$.

At a critical point of W , the potential (2.1) takes the form:

$$\mathcal{V} = -6W^2. \quad (4.28)$$

This nonpositive quantity gives the cosmological constant of AdS_5 , which is the supergravity solution at that point in the moduli space. With the choice of isometry given in (4.25), the flow between y_j and y_{j-1} interpolates between two AdS_5 solutions with the same value of the cosmological constant.

5. Examples

5.1 Models with $k > 1$ for low values of p

Models with $k = 1$ and negative $c_1(M)$ are very frequent: for each value of p , one obtains such a model by setting $q = 1$ (this leads to the Pedersen metrics [24], see below). Models with negative c_1 become increasingly sparse as one increases k . Let

us order all models increasingly by lexicographic order in (p, q) . Then it is not hard to check that a given value of k is first realized for $p/q = f_{2k+2}/f_{2k} = (3 \dots 3)$, where $f_1 = 1, f_2 = 1, f_3 = 2, f_4 = 3, f_5 = 5 \dots$ are the Fibonacci numbers. In particular,

- (a) $k = 2$ is first realized by $(p, q) = (8, 3)$
- (b) $k = 3$ is first realized by $(p, q) = (21, 8)$
- (c) $k = 4$ is first realized by $(p, q) = (55, 21)$
- (d) $k = 5$ is first realized by $(p, q) = (144, 55)$.

It is clear that one can realize any value of k (since finite minus continued fractions represent the rationals). We shall illustrate the general discussion of the previous section by giving a detailed analysis of Randall-Sundrum flows for the Pedersen metrics and for the models (a) and (b).

5.2 The Pedersen-LeBrun metrics

In [24], H. Pedersen constructed a one-dimensional family of $U(2)$ invariant ESD metrics of negative scalar curvature on the unit open four-ball B^4 . These metrics are characterized by a parameter¹⁵ $m^2 > -1$ which fixes their behavior near the S^3 boundary. In fact, the unit 3-sphere is a conformal infinity for these spaces, if the former is endowed with the Berger metric:

$$ds^2 = \sigma_1^2 + \sigma_2^2 + I_3 \sigma_3^2 \quad , \quad (5.1)$$

where $I_3 = \frac{1}{m^2+1} > 0$ and σ_i are three left-invariant one-forms on $S^3 = SU(2)$ such that $d\sigma_i = \epsilon_{ijk}\sigma_j \wedge \sigma_k$. These metrics are smooth and complete on B^4 for any $m^2 > -1$; their explicit form is given in Appendix A.

When $m^2 \in (-1, 0) \Leftrightarrow I_3 > 1$, these can be continued to complete metrics ‘on the other side’ of S^3 , provided that $|m| = \frac{p-2}{p}$ for some integer $p > 2$ [15]. In this case, the Pedersen ansatz and its continuation induce (up to a p -fold cover) smooth metrics on disjoint open subsets M_- and M_+ of the minimal resolution $M = \mathcal{O}(-p) \rightarrow \mathbf{P}^1$ of $\mathbf{C}^2/\mathbf{Z}_p$, where the generator of \mathbf{Z}_p acts through:

$$(z_1, z_2) \rightarrow (e^{2\pi i/p} z_1, e^{2\pi i/p} z_2) \quad . \quad (5.2)$$

These sets M_+ and M_- are separated by a common conformal infinity, namely the Lens space $Y = S^3/\mathbf{Z}_p$, carrying the conformal structure induced by the Berger metric. The conformal structures on M_+ and M_- agree along Y , and define a unique conformal structure on M ; the latter was discovered by LeBrun in the context of scalar-flat Kahler metrics [25].

¹⁵One allows m^2 to be positive or negative, so that m may be imaginary.

An interesting property of the Pedersen-LeBrun models is that they interpolate between the hyperbolic metric on B^4 and the Bergman metric¹⁶ [24]. The hyperbolic metric arises for $m = 0 \Leftrightarrow I_3 = 1$, while the Bergman space is obtained in the limit $m^2 \rightarrow -1 \Leftrightarrow I_3 \rightarrow \infty$. In the second case, the conformal structure induced on S^3 degenerates to a left-invariant CR structure [24, 15].

As shown in [15], the Pedersen-LeBrun metrics are the only smooth and complete ESD metrics of negative scalar curvature which admit a $U(2)$ isometry with 3-dimensional generic orbits. They form a special subclass in Hitchin's classification of complete and $SU(2)$ invariant ESD metrics. Since such metrics admit an obvious T^2 symmetry, they also fit into the framework of [10].

The Pedersen-LeBrun metrics were recently considered in [9], though in a different parameterization which originates in the work of [26]. Since the metrics of [9] are ESD and $U(2)$ -invariant of negative scalar curvature, Hitchin's classification assures us that they coincide with the Pedersen-LeBrun spaces. In appendix A, we give the explicit coordinate transformations which reduce the models of [9] to the Pedersen form.

By using their coordinates, the authors of [9] build a flow of Randall-Sundrum type on the subset M_+ of M for a certain choice of gauged isometry. In fact, the relevant isometry is the $U(1)$ factor in the decomposition $U(2) = U(1) \times SU(2)$. Since this is a subgroup of a $T^2 \subset U(2)$, it is natural to reconsider this problem from the point of view of the present paper. Below, we show how the flow of [9] can be recovered with our techniques.

In the framework of [22], the Pedersen metrics arise for $q = 1$. This immediately gives $k = 1$ and $e_1 = p$. Thus the exceptional divisor consists of a single two-sphere of self-intersection $-p$. The condition $p \geq 3$ implements the constraint $c_1(M) < 0$. The recursion relations (3.5) give:

$$(m_0, n_0) = (0, -1) \quad , \quad (m_1, n_1) = (1, 0) \quad , \quad (m_2, n_2) = (p, 1) \quad . \quad (5.3)$$

The toric generators of M for the case $p = 3$ are shown in figure 7.

¹⁶We remind the reader that the hyperbolic metric on B^4 is the homogeneous metric on the symmetric space $SO(4, 1)/SO(4)$ (also known as $EAdS_4$), while the Bergman metric is the homogeneous metric on $SU(2, 1)/U(2)$ (also known as the metric of the universal hypermultiplet).

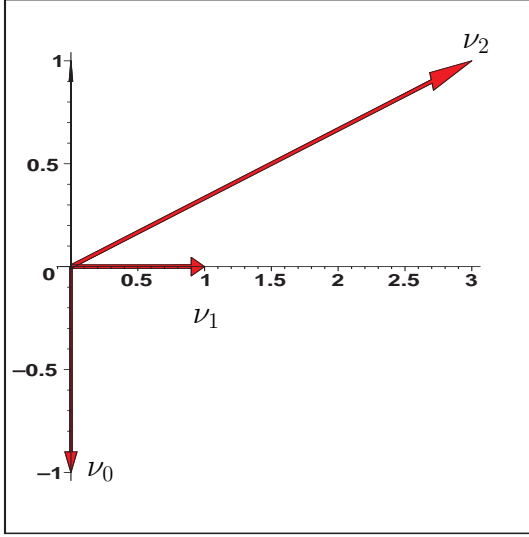


Figure 7: Toric generators ν_0, ν_1 and ν_2 for $(p, q) = (3, 1)$. The figure does not show the vector $\nu_3 = \begin{bmatrix} 0 \\ 1 \end{bmatrix}$ added when compactifying the minimal resolution.

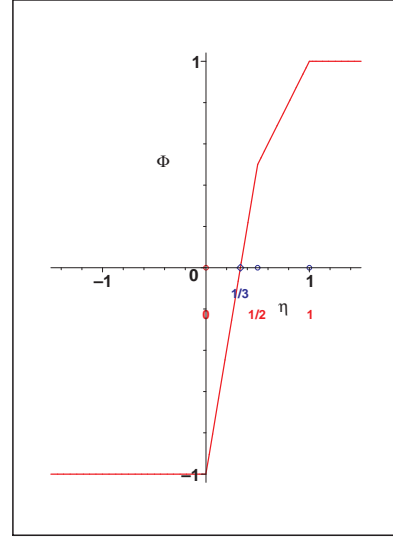


Figure 8: The function Φ for the model $(p, q) = (3, 1)$. The figure indicates the points $y_2 = 0, y_1 = 1/2$ and $y_0 = 1$, as well as the bordering value $\eta_0 = 1/3$.

One also has the formal pair $(m_3, n_3) = (0, 1)$. This gives:

$$y_0 = 1 \quad , \quad y_1 = \frac{1}{p-1} \quad , \quad y_2 = 0 \quad ; \quad \eta_0 = 1/p \quad (5.4)$$

and:

$$w_0 = -1/2 \quad , \quad w_1 = -(p-1)/2 \quad , \quad w_2 = p/2 \quad . \quad (5.5)$$

Hence the defining function F has the form:

$$F(\rho, \eta) = \frac{1}{2} \left[-f(\rho, \eta, 1) - (p-1)f(\rho, \eta, \frac{1}{p-1}) + pf(\rho, \eta, 0) \right] \quad . \quad (5.6)$$

The boundary $(1/p, \infty)$ of D_+ contains the points $y_0 = 1$ and $y_1 = 1/(p-1)$, while the point $y_2 = 0$ belongs to the boundary $(-\infty, 1/p)$ of D_- . The function Φ has the form:

$$\Phi(\eta) = \frac{1}{2} \left[-|\eta - 1| - (p-1)|\eta - \frac{1}{p-1}| + p|\eta| \right] \quad . \quad (5.7)$$

This is plotted in figure 8 (for the case $p = 3$). The isometry defined by $\lambda^{(1)} = 2/p$ has the property $W_0(y_1) = W_0(y_0) = \frac{1}{\sqrt{6}}(1 - 2/p)$. Figure 9 shows the level lines of the superpotential for $p = 3$ and $\lambda = \lambda^{(1)} = 2/3$.

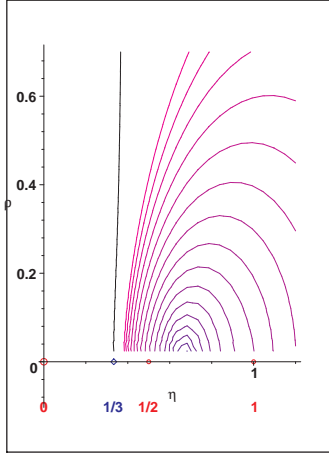


Figure 9: Level lines of the superpotential for $(p, q) = (3, 1)$ and $\lambda = 2/3$. In the color version of this figure, increasing values of W are represented by a red shift in the coloring of the level lines. The vertical bold black curve represents the conformal infinity Z . In this plot, we use the convention in which the superpotential is non-negative throughout D_+ .

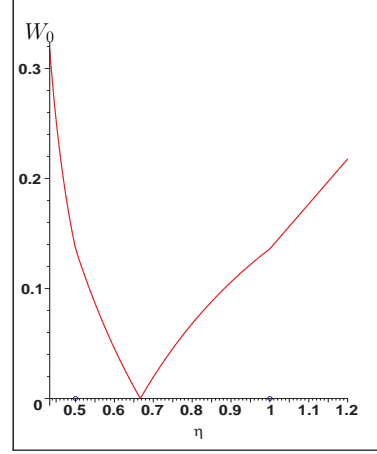


Figure 10: The restriction of W to the line $\rho = 0$ for $\lambda = 2/3$. The superpotential vanishes for $\eta = \lambda$.

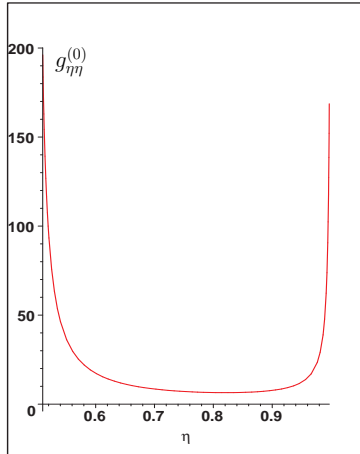


Figure 11: The restricted metric $g_{\eta\eta}^{(0)}$ for $(p, q) = (3, 1)$. As explained in the text, this is singular at $y_1 = 1/2$ and $y_0 = 1$.

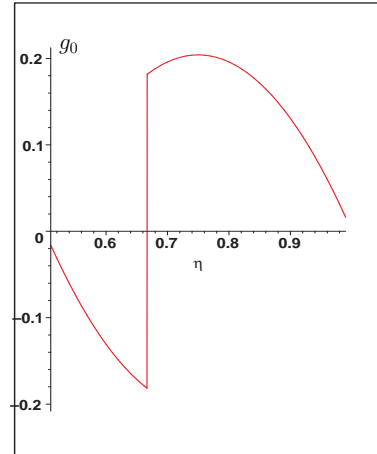


Figure 12: The restricted gradient field $g_0(\eta)$ for $(p, q) = (3, 1)$ and $\lambda = 2/3$. The vertical axis is measured in units of the coupling constant g . Note the discontinuity at $\eta = \lambda$. This is eliminated when considering the sign-corrected field $g_c(\eta)$ of equation (4.19).

The isometry fixing the interval $I_1 := (y_1, y_0) = (\frac{1}{p-1}, 1)$ has parameter $\lambda_1 = 0$. Therefore, the ϕ -circle collapses above this interval, while the fibration of the ψ -circle between y_1 and y_0 gives the exceptional divisor S_1 (this is the \mathbf{P}^1 base of the fibration $\mathcal{O}(-p) \rightarrow \mathbf{P}^1$).

On the interval I_1 , we have $\Phi(\eta) = \eta$ and $\Xi = m_1 = 1$. Therefore:

$$\begin{aligned} W_0(\eta) &= \frac{1}{\sqrt{6}} \frac{|\eta - \lambda|}{\eta} \\ g_0(\eta) &= -\lambda g \sqrt{6} \frac{(\eta - 1)((p - 1)\eta - 1)}{p - 2} . \end{aligned} \quad (5.8)$$

The sign-corrected functions W_c and g_c are plotted in figure 13.

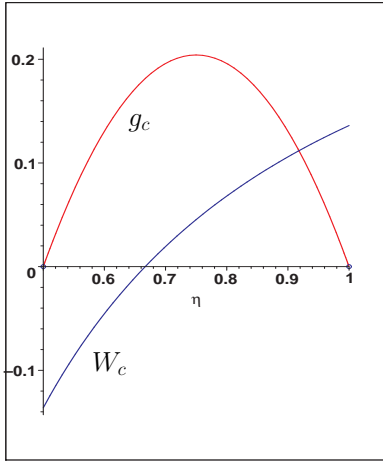


Figure 13: Sign-corrected superpotential W_c and gradient field g_c on the interval $(1/2, 1)$ (for $\lambda = 2/3$). Note continuity of g_c and the zero of W_c at $\eta = \lambda$.

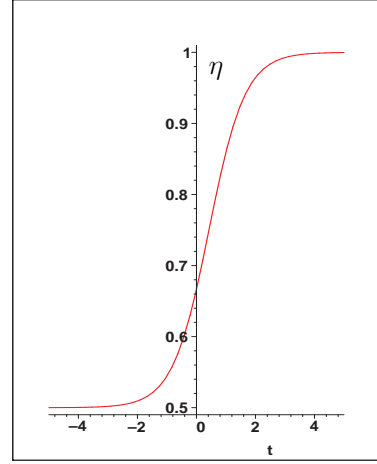


Figure 14: The flow $\eta(t)$ along the interval $(1/2, 1)$ for $(p, q) = (3, 1)$ and $\lambda = 2/3$. This flow is of Randall-Sundrum type.

The solution (4.22) takes the following form on the interval I_1 (if one chooses $\epsilon = +1$):

$$\frac{1}{2} \ln |\eta - 1| - \frac{1}{2} \ln \left| \eta - \frac{1}{p-1} \right| = -g \sqrt{\frac{3}{2}} \lambda t . \quad (5.9)$$

Upon clearing denominators in the logarithms and absorbing the resulting constant by a shift of t (see the footnote after equation (4.22)), we obtain $\ln((p-1)\eta-1) - \ln(1-\eta) = g\lambda\sqrt{6}t$, which gives:

$$\eta(t) = \frac{e^{-\lambda\sqrt{6}gt} + 1}{(p-1)e^{-\lambda\sqrt{6}gt} + 1}$$

$$U(t) = -\frac{1}{6} \left[(p-2) \ln(e^{-\lambda\sqrt{6}gt} + 1) - (\lambda-1)\sqrt{6}gt \right] . \quad (5.10)$$

(this solution satisfies $\eta(-\infty) = y_1 = \frac{1}{p-1}$ and $\eta(+\infty) = y_0 = 1$). $\eta(t)$ is plotted in figure 14 for $p = 3$ and $\lambda = 2/3$. For $\lambda = \lambda^{(1)} = 2/p$, the solution for U becomes:

$$U(t) = -\frac{p-2}{6} \ln \left[2 \cosh\left(\frac{\sqrt{6}}{p}gt\right) \right] . \quad (5.11)$$

For each $\lambda \in I_1$, the flow (5.10) has Randall-Sundrum type and proceeds along a meridian of the two-sphere S_1 (figure 15).

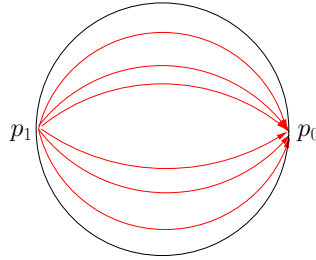


Figure 15: Divisorial flows for the Pedersen models. The flows proceed along the meridians of the \mathbf{P}^1 base of M , between the two critical points located at the poles p_1, p_0 . The interval $I_1 = (\frac{1}{p-1}, 1)$ sits along the axis connecting these poles.

Let us discuss the relation with [9]. Since we don't know the explicit coordinate transformation between the Calderbank-Pedersen metric (2.4) and the parameterization used in [9], we cannot immediately compare our solution for η with the solution for their coordinate x . However, we can compare the warp factors, since in both cases they depend only on the fifth space-time coordinate (denoted by ρ in [9] and by t in the present paper). The solution given in equation (94) of [9] has the form:

$$e^{2U(\rho)} = [\cosh(2g\rho)]^{-\frac{2}{3}(n-r_-)(n+r_+)} , \quad (5.12)$$

where $r_{\pm} = -n \pm \sqrt{4n^2 - 1}$ ¹⁷. So $(n - r_-)(n + r_+) = (2n + \sqrt{4n^2 - 1})\sqrt{4n^2 - 1}$. Our solution (5.11) gives:

$$e^{2U(t')} = 2^{\frac{2-p}{3}} [\cosh(2gt')]^{-\frac{p-2}{3}} , \quad (5.13)$$

where we have rescaled $t' = \frac{\sqrt{6}t}{2p}$, which should be identified with the coordinate ρ of [9]. This change of scale is due to the different normalization chosen in [9] for the Killing

¹⁷Equation (94) of [9] actually reads $e^{2U(\rho)} = [\cosh(2g\rho)]^{-\frac{1}{3}(n-r_-)(n+r_+)}$. The missing factor of 2 in the exponent is due to a typo in [9], as one can check that equations (91), (92) and (93) of that paper give $e^{U(\rho)} = [\cosh(2g\rho)]^{-\frac{1}{3}(n-r_-)(n+r_+)}$. We also note a missing factor of g in the RHS of the first equation (92) of [9].

vector (2.17). Together with the power of two prefactor in (5.13), this can be absorbed into a constant rescaling of the spacetime metric (2.15), as explained in the observation following equation (2.17).

Hence to compare the solutions we must compare the exponents in (5.12) and (5.13). Using $p = \frac{2}{1-|m|}$ and the relation $m^2 = -(1 - \frac{1}{4n^2})$, we obtain:

$$p = \frac{2}{1 - \sqrt{1 - \frac{1}{4n^2}}} = \frac{4n}{2n - \sqrt{4n^2 - 1}}. \quad (5.14)$$

Hence

$$p - 2 = \frac{2\sqrt{4n^2 - 1}}{2n - \sqrt{4n^2 - 1}} = \frac{2\sqrt{4n^2 - 1}(2n + \sqrt{4n^2 - 1})}{4n^2 - (4n^2 - 1)} = 2\sqrt{4n^2 - 1}(2n + \sqrt{4n^2 - 1}). \quad (5.15)$$

This agrees with the exponent of (5.12).

5.3 The model $(p,q)=(8,3)$

In this case, the Calderbank-Singer metric is defined on the minimal resolution of the orbifold $\mathbf{C}^2/\mathbf{Z}_8$ with action:

$$(z_1, z_2) \rightarrow (e^{\pi i/4} z_1, e^{3\pi i/4} z_2) . \quad (5.16)$$

The intersection matrix of the exceptional \mathbf{P}^1 's is given by (3.2), with the integers e_j determined by the continued fraction expansion:

$$p/q = 8/3 = (3, 3) = 3 - \frac{1}{3} . \quad (5.17)$$

The minimal resolution has negative c_1 since $e_1, e_2 \geq 3$. The model has $k = 2$, which gives four distinguished points $y_0 \dots y_{k+1}$ on the conformal boundary of \mathcal{H}^2 . Solving the recursion relations (3.5) gives: $(m_0, n_0) = (0, -1)$, $(m_1, n_1) = (1, 0)$, $(m_2, n_2) = (3, 1)$ and $(m_3, n_3) = (8, 3)$. As explained above, one also adds the formal values $(m_4, n_4) = (0, 1)$. The quantities $y_0 \dots y_3$ and $w_0 \dots w_3$ are given by (3.8):

$$\begin{aligned} (y_0 \dots y_3) &= (1, 1/2, 2/5, 1/4) \\ (w_0 \dots w_3) &= (-1/2, -1, -5/2, 4) . \end{aligned} \quad (5.18)$$

The conformal boundary $Z = \{F = 0\}$ meets the real axis in the point $\eta_0 = q/p = 3/8$. The spheres S_1, S_2 are fixed by the isometries defined by the following values of λ :

$$(\lambda_0 \dots \lambda_4) = (-\infty, 0, 1/3, 3/8, \infty) . \quad (5.19)$$

The toric generators $\nu_0 \dots \nu_3$ are shown in figure 1 of Section 3. The exceptional divisor of such models consists of two spheres S_1 and S_2 , associated with the intervals $I_1 = (y_1, y_0) = (1/2, 1)$ and $I_2 = (y_2, y_1) = (2/5, 1/2)$ (figure 16). Figures 17 and 18 show the level lines of the superpotential for $\lambda = 2/3$ and $\lambda = 3/7$.

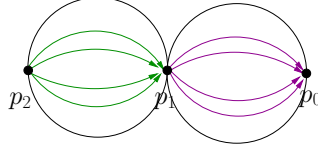


Figure 16: The exceptional divisor for $(p, q) = (8, 3)$. The Randall-Sundrum flows constructed below proceed along the meridians of one of the spheres.

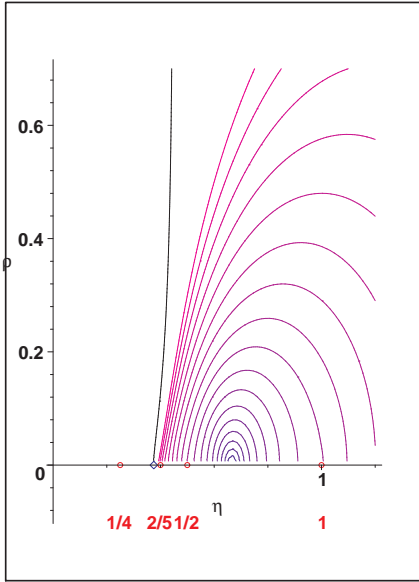


Figure 17: Level lines of the superpotential for $(p, q) = (8, 3)$ and $\lambda = 2/3$. Increasing values of W are represented by a red shift in the coloring of the level lines. The vertical bold black curve represents the conformal infinity Z . The superpotential is taken to be non-negative throughout D_+ .

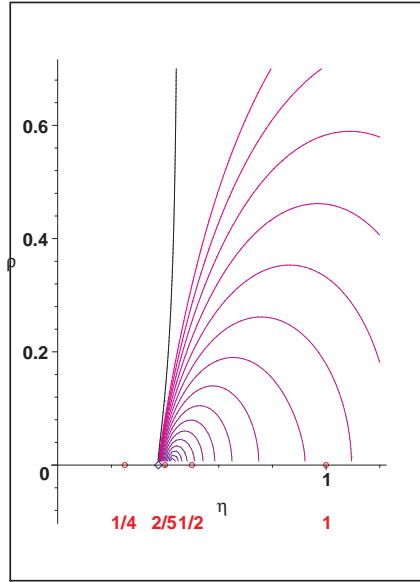


Figure 18: Level lines of the superpotential for $(p, q) = (8, 3)$ and $\lambda = 3/7$.

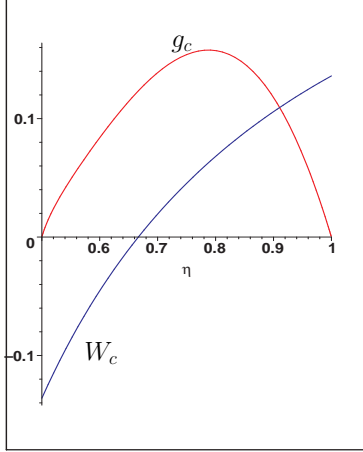


Figure 19: Sign-corrected superpotential and gradient field g_0 on the interval $(1/2, 1)$ for $\lambda = 2/3$.

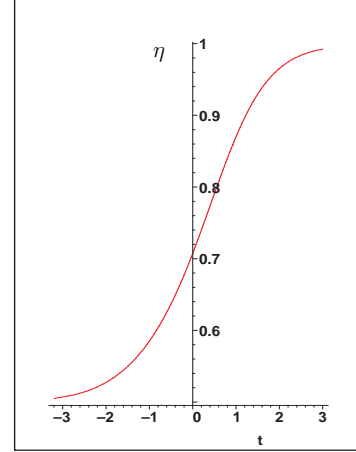


Figure 20: Flow along the interval $I_1 = (1/2, 1)$ for $\lambda = 2/3$.

To find a Randall-Sundrum flow on the interval $I_1 = (1/2, 1)$, we pick a value for $\lambda \in I_1$ and compute the form of the gradient field $g_0(\eta)$ of equation (4.7) along this interval. Taking into account the sign prefactors, one obtains:

$$g_0(\eta) = -\lambda g \sqrt{6} \frac{(\eta - 1)(2\eta - 1)(5\eta - 2)(4\eta - 1)}{8\eta^2 + 5\eta - 4} . \quad (5.20)$$

The solution of (4.10) is given implicitly by the equation:

$$\ln(1 - \eta) - \ln(2\eta - 1) - 2\ln(5\eta - 2) + 2\ln(4\eta - 1) = -\lambda \sqrt{6} g t , \quad (5.21)$$

where we used the freedom to shift t in order to absorb a term $\ln\left(\frac{25}{8}\right)$ from the left hand side. This solution is plotted in figure 20 for the choice $\lambda = 2/3$, which ensures $-W_0(1/2) = W_0(1) = \frac{1}{3\sqrt{6}}$. The full flow proceeds along some fixed meridian of the sphere S_1 .

For $\lambda, \eta \in I_2 = (2/5, 1/2)$, one obtains:

$$g_0(\eta) = -g \sqrt{6} \frac{(3\lambda - 1)(\eta - 1)(2\eta - 1)(5\eta - 2)(4\eta - 1)}{64\eta^2 - 59\eta + 13} , \quad (5.22)$$

with sign-corrected superpotential $W_0(\eta) = \frac{1}{\sqrt{6}} \frac{\eta - \lambda}{3\eta - 1}$.

The divisorial flow $\eta(t)$ is given by the equation:

$$-2\ln(1 - \eta) - \ln(1 - 2\eta) + \ln(5\eta - 2) + 2\ln(4\eta - 1) = (3\lambda - 1)\sqrt{6} g t . \quad (5.23)$$

This flow is plotted in figure 22, for $\lambda = 3/7$. With this value of λ , one has $-W_0(2/5) = W_0(1/2) = \frac{\sqrt{6}}{42}$. The full flow proceeds along some fixed meridian of the sphere S_2 .

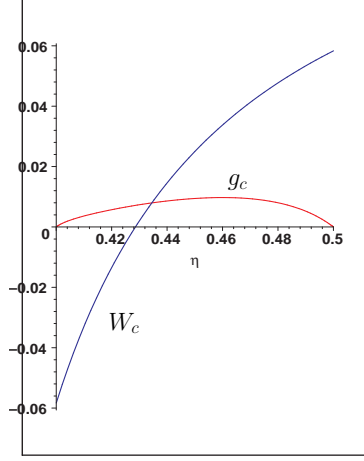


Figure 21: Sign-corrected superpotential and gradient field g_0 on the interval $I_2 = (2/5, 1/2)$ (for $\lambda = 3/7$).

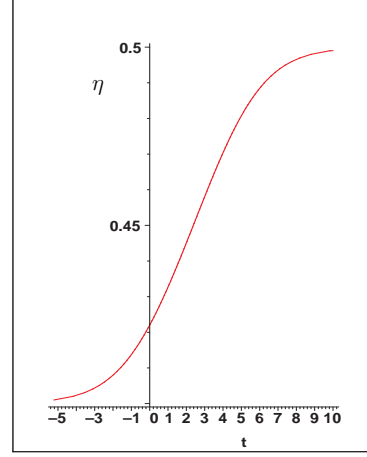


Figure 22: Flow along the interval $I_2 = (2/5, 1/2)$ for $\lambda = 3/7$.

5.4 The model $(p,q)=(21,8)$

In this case, we have $k = 3$ and $e_1 = e_2 = e_3 = 3$. The recursions (3.5) give:

$$\begin{aligned} (m_0 \dots m_5) &= (0, 1, 3, 8, 21, 0) \\ (n_0 \dots n_5) &= (-1, 0, 1, 3, 8, 1) \quad . \end{aligned} \quad (5.24)$$

The curve Z intersects the line $\rho = 0$ at $\eta_0 = 8/21$. One easily computes:

$$\begin{aligned} (y_0 \dots y_4) &= (1, 1/2, 2/5, 5/13, 1/3) \\ (w_0 \dots w_4) &= (-1/2, -1, -5/2, -13/2, 21/2) \\ (\lambda_1 \dots \lambda_4) &= (0, 1/3, 3/8, 8/21) \quad . \end{aligned} \quad (5.25)$$

The function Φ for this model is shown in figure 24 below. The points $(y_0 \dots y_3) = (1, 1/2, 2/5, 5/13)$ belong to D_+ , while $y_4 = 1/3$ (added when compactifying the minimal resolution) belongs to D_- . The boundary of D_+ contains three finite length intervals $I_1 = (1/2, 1)$, $I_2 = (2/5, 1/2)$ and $I_3 = (5/13, 2/5)$. One obtains flows of Randall-Sundrum type along these intervals (with equal values of W at the endpoints of the flow) for the following values of λ (see equation (4.25)):

$$(\lambda^{(1)}, \lambda^{(2)}, \lambda^{(3)}) = (2/3, 3/7, 7/18) \quad . \quad (5.26)$$

Equation (4.22) gives the following expressions for the Randall-Sundrum flows along these intervals:

$$\begin{aligned}
I_1 : & \ln(1 - \eta) - \ln(2\eta - 1) - 2 \ln(5\eta - 2) - 5 \ln(13\eta - 5) + 7 \ln(3\eta - 1) \\
& = -g\sqrt{6}\lambda t \\
I_2 : & 2 \ln(1 - \eta) + \ln(1 - 2\eta) - \ln(5\eta - 2) - 2 \ln(13\eta - 5) \\
& = -g\sqrt{6}(3\lambda - 1)t \\
I_3 : & 5 \ln(1 - \eta) + 2 \ln(1 - 2\eta) - \ln(2 - 5\eta) - \ln(13\eta - 5) - 7 \ln(3\eta - 1) \\
& + = -g\sqrt{6}(8\lambda - 3)t.
\end{aligned} \tag{5.27}$$

The geometry of these flows is shown in figure 23. Figures 25, 26 and 27 plot the solutions (5.27) for the values of λ given in (5.26). From (4.26) we find the superpotentials: $W_0^{(I_1)}(1) = \frac{1}{3\sqrt{6}}$, $W_0^{(I_2)}(\frac{1}{2}) = \frac{1}{7\sqrt{6}}$, $W_0^{(I_3)}(\frac{2}{5}) = \frac{1}{18\sqrt{6}}$.

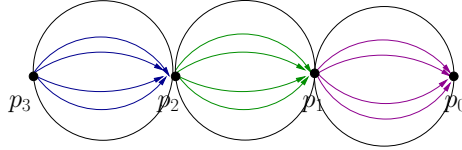


Figure 23: Randall-Sundrum flows for $(p, q) = (21, 8)$.

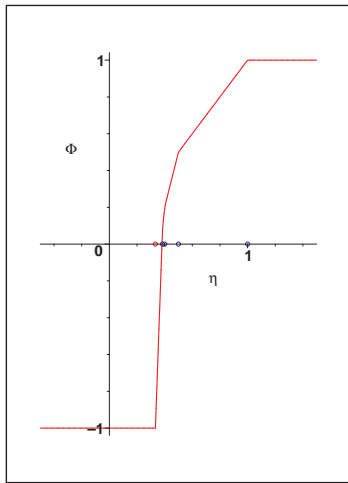


Figure 24: The function Φ for $(p, q) = (21, 8)$.

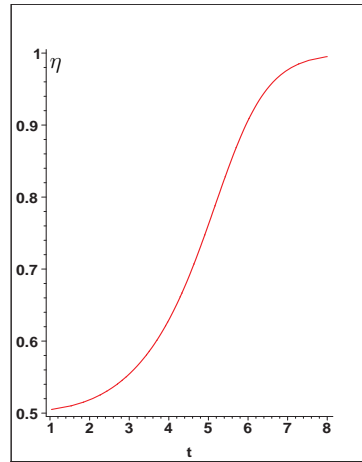


Figure 25: Flow of Randall-Sundrum type for $\lambda = 2/3$.

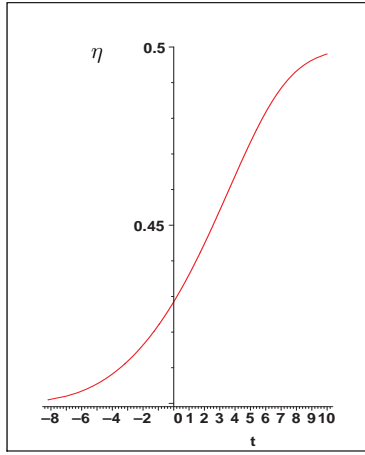


Figure 26: Flow of Randall-Sundrum type for $\lambda = 3/7$.

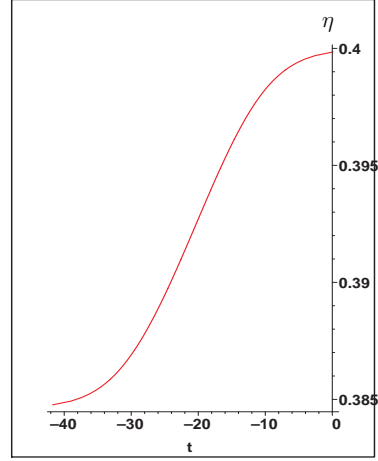


Figure 27: Flow of Randall-Sundrum type for $\lambda = 7/18$.

6. Conclusions

We constructed an infinite family of gauged N=2 supergravities in 5 dimensions admitting Randall-Sundrum flows. The matter content of these models consists of a single hypermultiplet described by the complete and smooth quaternion-Kähler four-manifolds constructed recently by Calderbank and Singer. These metrics are defined on an open subset of the minimal resolution of a cyclic singularity, and have negative scalar curvature provided that this resolution has negative definite first Chern class. They admit a T^2 's worth of isometries and generalize the well-known Pedersen metrics [24], which admit a larger $U(2)$ symmetry.

By using the coordinates of [10], we found a very simple expression for the superpotential obtained by gauging one of the toric isometries, and showed that the associated flow preserves each of the two-spheres which form the irreducible components of the exceptional divisor. Moreover, the restriction of the flow to the exceptional divisor can be described by a simple ordinary differential equation, which can be integrated by quadratures. We also showed that the restriction of the flow to each given sphere is of Randall-Sundrum type for an appropriate range of choices of the gauged isometry. The models obtained in this manner allow for an arbitrary number of critical points.

For a few models in this class, we performed a detailed study of such ‘divisorial’ flows and gave explicit constructions in the Randall-Sundrum case. Finally, we pointed out that the models considered recently in [9] are the well-known Pedersen metrics, albeit discussed in a different parameterization. They form the simplest case of the family analyzed in the present paper. Clearly our models give an infinite number of

counterexamples to the no-go theorems mentioned in the introduction. As in [9], the reason is very simple: such theorems were formulated for supergravity coupled only to vector/tensor multiplets or they assumed homogeneity of the hypermultiplet moduli space. Finally, the result of [8] relies on non-positivity assumptions for the scalar potential which fail to hold along our flows: one has $\mathcal{V} > 0$ when the flow passes through the zero of W .

It would be interesting to study possible RG flow interpretations of the domain wall solutions interpolating between UV and IR critical points, which were also found in the present paper. A more challenging question is whether our models embed consistently in string/M-theory.

Acknowledgments

The authors thank M. Roček for support and interesting conversations. This work was supported by the Research Foundation under NSF grant PHY-0098527.

A. Relation between different coordinate systems for the Pedersen metrics

The Pedersen metric [24] has the form:

$$g = \frac{1}{(1 - \rho^2)^2} \left[\frac{1 + m^2 \rho^2}{1 + m^2 \rho^4} d\rho^2 + \rho^2 (1 + m^2 \rho^2) (\sigma_1^2 + \sigma_2^2) + \frac{\rho^2 (1 + m^2 \rho^4)}{1 + m^2 \rho^2} \sigma_3^2 \right], \quad (\text{A.1})$$

where σ_i are the standard $SU(2)$ left-invariant one-forms, obeying $d\sigma_i = \epsilon_{ijk} \sigma_j \wedge \sigma_k$:

$$\begin{aligned} \sigma_1 &= \frac{1}{2} (-\sin \psi d\theta + \cos \psi \sin \theta d\phi) \\ \sigma_2 &= \frac{1}{2} (\cos \psi d\theta + \sin \psi \sin \theta d\phi) \\ \sigma_3 &= \frac{1}{2} (d\psi + \cos \theta d\phi) \end{aligned} \quad (\text{A.2})$$

with $0 \leq \theta < \pi$, $0 \leq \phi < 2\pi$ and $0 \leq \psi < 4\pi$. Clearly $\sigma_1^2 + \sigma_2^2 = \frac{1}{4}(d\theta^2 + \sin^2 \theta d\phi^2)$.

Behrndt and Dall'Agata give several different parameterizations of their metric and also the coordinate transformations between them. For convenience, let us take the parameterization (43) of [9]¹⁸:

$$ds^2 = \frac{dr^2}{V(r)} + V(r)(d\tau + 2n \cos \theta d\phi)^2 + (r^2 - n^2)(d\theta^2 + \sin^2 \theta d\phi^2),$$

¹⁸This form of the metric is valid only when the parameter κ of [9] equals one, which is exactly the case we are interested in.

$$V(r) = \frac{r-n}{r+n} [(r+n)^2 + 1 - 4n^2]. \quad (\text{A.3})$$

One obtains (A.1) from (A.3) by the following coordinate transformation:

$$r = \frac{\rho^2}{2n(1-\rho^2)} + n, \quad \tau = 2n\psi \quad (\text{A.4})$$

and the identification $m^2 = \frac{1}{4n^2} - 1$. Actually doing this results in four times the metric (A.1). But this was to be expected since the scalar curvature of (A.3) is normalized to -12 , whereas Pedersen [24] normalizes the cosmological constant to -12 (i.e. the scalar curvature to $-12 \times 4 = -48$). The extra factor of 4 coming as a result of the coordinate transformation (A.4) accounts for that difference.

Taking $n = 1/2$ in the metric (A.3) and performing the coordinate transformation (A.4) again with $n = 1/2$ one obtains:

$$\frac{4}{(1-\rho^2)^2} [d\rho^2 + \rho^2(\sigma_1^2 + \sigma_2^2 + \sigma_3^2)], \quad (\text{A.5})$$

which is the metric of Euclidean AdS_4 space, normalized so that the scalar curvature is -12 . The same metric (A.5) (without the factor of 4) one obtains from (A.1) upon setting $m = 0$.

Another form of the Pedersen metric is [15]:

$$g = \frac{1}{(\cos \rho' - M \sin \rho')^2} \left[(1 + M \cot \rho') [d\rho'^2 + 4 \sin^2 \rho' (\sigma_1^2 + \sigma_2^2)] + \frac{4M^2}{1 + M \cot \rho'} \sigma_3^2 \right]. \quad (\text{A.6})$$

Its relation to (A.1) is given by:

$$\cos \rho' = \frac{1}{\sqrt{1 + \frac{\rho^4}{M^2}}}, \quad M = \frac{1}{m}. \quad (\text{A.7})$$

Again one obtains four times (A.1) due to different normalizations between [24] and [15].

References

- [1] A. Lukas, B. Ovrut, K. Stelle, D. Waldram, *The Universe as a Domain Wall*, Phys. Rev. **D59** (1999) 086001, hep-th/9803235
- [2] P. Horava, E. Witten, *Heterotic and Type I String Dynamics from Eleven Dimensions*, Nucl. Phys. **B460** 506, hep-th/9510209

- [3] E. Witten, *Strong coupling expansion of Calabi-Yau compactification*, Nucl.Phys. **B471**(1996) 135, hep-th/9602070.
- [4] J. Maldacena, *The Large N Limit of Superconformal Field Theories and Supergravity*, Adv. Theor. Math. Phys. **2** (1998) 231, hep-th/9711200
- [5] L. Randall, R. Sundrum, *An alternative to compactification*, Phys. Rev. Lett. **83** (1999) 4690, hep-th/9906064.
- [6] R. Kallosh, A. Linde, *Supersymmetry and the Brane World*, JHEP **02**, (2000) 005, hep-th/0001071
- [7] G. Gibbons, N. Lambert, *Domain Walls and Solitons in Odd Dimensions*, Phys. Lett. **488** (2000) 90, hep-th/0003197
- [8] J. Maldacena, C. Nunez, *Supergravity Description of Field Theories on Curved Manifolds a no-go Theorem*, Int. J. Mod. Phys. **A16** (2001) 822, hep-th/0007018
- [9] K. Behrndt, G. Dall'Agata, *Vacua of $N=2$ gauged supergravity derived from non-homogeneous quaternionic spaces*, Nucl.Phys. B627 (2002) 357-380, hep-th/0112136.
- [10] D. M. J. Calderbank, H. Pedersen, *Selfdual Einstein metrics with torus symmetry*, math-dg/0105263.
- [11] A. Ceresole, G. Dall'Agata *General matter coupled $N = 2$, $D = 5$ gauged supergravity*, hep-th/0004111.
- [12] A. Ceresole, G. Dall'Agata, R. Kallosh, A. Van Proeyen *Hypermultiplets, Domain Walls and Supersymmetric Attractors*, hep-th/0104056.
- [13] D. V. Alekseevsky, V. Cortes, C. Devchand, A. Van Proeyen, *Flows on quaternionic-Kaehler and very special real manifolds*, hep-th/0109094.
- [14] R. D'Auria, S. Ferrara *On Fermion Masses, Gradient Flows and Potential in Supersymmetric Theories*, hep-th/0103153.
- [15] N. Hitchin, *Twistor spaces, Einstein metrics and isomonodromic deformations*, J. Diff. Geom. **42**(1995)30-112.
- [16] K. Galicki, H. B. Lawson, Jr, *Quaternionic reduction and quaternionic orbifolds*, Math. Ann. **282** (1988) 1-21.
- [17] R. L. Bryant, S. M. Salamon, *On the construction of some complete metrics with exceptional holonomy*, Duke Math. J. **58** (1989)3, 829.
- [18] L. Anguelova, C. I. Lazaroiu, *M-theory compactifications on certain 'toric' cones of G_2 holonomy*, hep-th/0204249.

- [19] L. Anguelova, C.I. Lazaroiu, *M-theory on 'toric' G_2 cones and its type II reduction*, hep-th/0205070.
- [20] B. Acharya, E. Witten, *Chiral Fermions from Manifolds of G_2 Holonomy*, hep-th/0109152.
- [21] G. W. Gibbons, D. N. Page, C. N. Pope, *Einstein metrics on S^3 , \mathbf{R}^3 and \mathbf{R}^4 bundles*, Commun. Math. Phys **127** (1990), 529-553.
- [22] D. Calderbank, M. A. Singer, *Einstein metrics and complex singularities*, math-dg/0206229.
- [23] T. Eguchi, A. Hanson, *Asymptotically Flat Self-Dual Solutions to Euclidean Gravity*, Phys. Lett. **74B** (1978) 249; G. Gibbons, S. Hawking, *Gravitational Multi-Instantons*, Phys. Lett. **78B** (1978) 430.
- [24] H. Pedersen, *Einstein metrics, spinning top motions and monopoles*, Math. Ann. **274** (1986) 35-39.
- [25] C. R. LeBrun, *Counterexamples to the generalized positive action conjecture*, Commun. Math. Phys, **118** (1988) 591-596.
- [26] D. N. Page, C. N. Pope, *Inhomogeneous Einstein metrics on complex line bundles*, Class. Quant. Grav. **4** (1987) 213.
- [27] W. Barth, C. Peters, A.V. de Wen, *Compact Complex Surfaces*, Springer-Verlag, 1984.
- [28] V. Danilov, *The geometry of toric varieties*, Russian Math. Surveys **33:2**(1978), 97.
- [29] T. Oda, *Convex bodies and algebraic geometry. An introduction to the theory of toric varieties*. Ergebnisse der Mathematik und ihrer Grenzgebiete, 15. Springer-Verlag, Berlin, 1988.
- [30] W. Fulton, *Introduction to toric varieties*, Annals of mathematics studies no. **131**, Princeton University Press, 1993.
- [31] M. Audin, *The topology of torus actions on symplectic manifolds*, Progress in Math. **93**, Birkhauser, 1991.
- [32] K. Behrndt, *Domain walls and flow equations in supergravity*, Fortsch.Phys. **49** (2001) 327-338, hep-th/0101212.
- [33] M. Gunaydin, L. J. Romans, N. P. Warner, *Gauged $N = 8$ Supergravity in Five Dimensions*, Phys. Lett. **B154** (1985) 268.
- [34] M. Pernici, K. Pilch, P. van Nieuwenhuizen, *Gauged $N = 8$ $D = 5$ Supergravity*, Nucl. Phys. **B259** (1985) 460.

- [35] A. Khavaev, K. Pilch, N. P. Warner, *New vacua of gauged $N = 8$ supergravity in five dimensions*, Phys. Lett. **B487** (2000) 14, hep-th/9812035.
- [36] M. Cvetič et al., *Embedding AdS Black Holes in ten and Eleven Dimensions*, Nucl. Phys. **B558** (1999) 96, hep-th/9903214.
- [37] B. de Wit, H. Nicolai, *The Consistency of the S^7 Truncation in $d = 11$ Supergravity*, Nucl. Phys. **B281** (1987) 211.
- [38] H. Nastase, D. Vaman, P. van Nieuwenhuizen, *Consistent nonlinear KK reduction of 11d supergravity on $AdS_7 \times S^4$ and self-duality in odd dimensions*, Phys. Lett. **B469** (1999) 96, hep-th/9905075; *Consistency of the $AdS_7 \times S^4$ reduction and the origin of self-duality in odd dimensions*, Nucl. Phys. **B581** (2000) 179, hep-th/9911238.
- [39] D. Z. Freedman, S. S. Gubser, K. Pilch, N. P. Warner, *Renormalization Group Flows from Holography – Supersymmetry and a c-Theorem*, Adv. Theor. Math. Phys. **3** (1999) 363, hep-th/9904017.
- [40] L. Girardello, M. Petrini, M. Porrati, A. Zaffaroni, *The Supergravity Dual of $N = 1$ Super Yang-Mills Theory*, Nucl. Phys. **B569** (2000) 451, hep-th/9909047.